POLITECNICO DI TORINO

Corso di Laura Magistrale

in Ingegneria Meccanica

Tesi di Laurea Magistrale

Fuel identification control strategy based on in-cylinder pressure sensor

Relatore

Prof. Federico Millo

Candidato

Davide Zanco

Anno Accademico 2019/2020

Acknowledgments

As expected, there are many people to whom I have to thank for their support during my university studies. I am grateful to all those who have contributed to the work described in this thesis or to me personally during the time spent working on it.

First of all, I must thank Professor Federico Millo for the opportunity given to carry out this experience. In addition, I must acknowledge the contributions of engineer Matteo Mautino, company supervisor, who has provided substantial guidance from the beginning of the path within the company. I am grateful for his continued support and important help in the thesis work for engineer Vivek Srivastava. I am also grateful for the technical reviews, planning and intellectual advice offered by project leader Dr. Christian Jorg.

Last but certainly not least, I would like to thank my family: my parents, Debora, Gionata and Ilaria, who have pushed me over the years and whose support has been absolutely essential.

Abstract

The increasing demands placed on the powertrain community to develop propulsion systems with higher fuel efficiency has led to advanced technologies targeting a continuous improvement of the engine's thermal efficiency, while maintaining low pollutants emissions' levels. Additionally, the development of fuels that provide improved combustion and reduce the overall emission footprint is gaining increasing importance. It is therefore critical to understand how the combustion responds to variations in fuel properties, especially the cetane number, the primary quantification of ignition behavior.

With the introduction of new fuels, such as vegetable oils, it has become necessary to identify the fuel quality in use inside the engine if two or more fuels are available on board. This is possible through the use of new technologies such as fuel sensors. An alternative strategy is to use an in-cylinder pressure sensor to optimize combustion behavior with a closed loop control.

This study analyzes strategies to identify the fuel through combustion characteristics based on in-cylinder pressure sensors such as ignition delay, start of combustion, phasing, pressure gradient. First of all, the correlation between fuel properties, in particular cetane number, and the combustion is studied. Ignition delay and start of combustion were found to be dependent on fuel cetane number: increasing cetane number advances start of combustion and reduces ignition delay. This is related to the definition of cetane number, which indicates the measure of how readily the fuel starts to burn (autoignites). A sensitivity analysis was subsequently carried out; it was found that ignition delay is a more suitable indicator than start of combustion because it is less sensitive then start of combustion.

Once the influence of the fuel properties on the combustion characteristics was found, it was analyzed which strategy is the most suitable to identify the fuel; the cetane number derived from ignition delay can be obtained either at specific engine operation points or under certain thermodynamic conditions. In addition, to predict ignition delay a model has been added in order to provide greater accuracy and reduce calibration efforts. This has allowed to predict ignition delay in a wider range of conditions. The result is that using specific speed and load to obtain ignition delay could lead to errors due to different environmental conditions, while the thermodynamic conditions criteria shows a higher robustness in the calculation of ignition delay and consequently in predicting the cetane number.

The results obtained with the fuel identification algorithm have been validated with a pressure sensor drift simulation and a signal noise model. The disturbance simulations were modelled experimentally from real data of the pressure sensor behavior. It was found that even with sensor drift in combination with signal noise under common operating conditions the deviation of the predicted cetane number did not exceed 4, which is small enough to identify two distinct fuels.

Abstract

Le crescenti richieste di sistemi di propulsione con una maggiore efficienza e le normative sempre più stringenti hanno portato a tecnologie avanzate che mirano ad un continuo miglioramento dell'efficienza termica del motore, pur mantenendo bassi i livelli di emissioni inquinanti. Inoltre, lo sviluppo di combustibili alternativi che garantiscano una migliore combustione e riducano le emissioni sta acquisendo sempre maggiore importanza. È quindi fondamentale capire come la combustione risponde alle variazioni delle proprietà del combustibile.

Con l'introduzione di nuovi combustibili, come gli oli vegetali, e la differente qualità del Diesel nelle diverse nazioni è diventato necessario identificare la qualità del combustibile in uso all'interno del motore. Ciò è possibile attraverso l'uso di nuove tecnologie come i sensori in grado di identificare il combustibile oppure tramite una strategia alternativa che è quella di utilizzare un sensore di pressione all'interno della camera per ottimizzare il comportamento della combustione con un controllo a circuito chiuso.

Questo studio analizza le strategie per identificare il combustibile attraverso le caratteristiche di combustione basate sui sensori di pressione della camera, come il ritardo di accensione, l'inizio della combustione, la fasatura, il gradiente di pressione. Prima di tutto viene studiata la correlazione tra le proprietà del combustibile, in particolare il numero di cetano, e la combustione. Il ritardo di accensione e l'inizio della combustione sono risultati dipendenti dal numero di cetano del combustibile: l'aumento del numero di cetano fa anticipare l'inizio della combustione e riduce il ritardo di accensione. Ciò è legato alla definizione di numero di cetano, che indica la misura della reattività del combustibile a bruciare (auto accensione). Successivamente è stata effettuata un'analisi di sensibilità: si è constatato che il ritardo di accensione è un indicatore più adatto rispetto all'inizio della combustione perché è meno sensibile rispetto all'inizio della combustione.

Una volta trovata l'influenza delle proprietà del combustibile sulle caratteristiche della combustione, è stata analizzata la strategia più adatta per identificare il combustibile. Il numero di cetano derivato dal ritardo di accensione può essere ottenuto sia in specifici punti di funzionamento del motore che in determinate condizioni termodinamiche. Inoltre, per prevedere il ritardo di accensione è stato aggiunto un modello per fornire una maggiore precisione e ridurre gli sforzi di calibrazione. Ciò ha permesso di prevedere il ritardo di accensione in una gamma più ampia di condizioni. Il risultato è che l'utilizzo della velocità del motore e del carico come criterio per ottenere il ritardo di accensione potrebbe portare ad errori dovuti a diverse condizioni ambientali, mentre il criterio delle condizioni termodinamiche mostra una maggiore robustezza nel calcolo del ritardo di accensione e di conseguenza nella previsione del numero di cetano.

I risultati ottenuti con l'algoritmo di identificazione del combustibile sono stati validati con una simulazione della deriva del sensore di pressione e un modello di rumore del segnale. Le simulazioni di disturbo sono state modellate sperimentalmente a partire da dati reali del comportamento del sensore di pressione. Si è scoperto che anche con la deriva del sensore in combinazione con il rumore del segnale in condizioni operative comuni la deviazione del numero di cetano previsto non superava 3, il quale è abbastanza basso da identificare due combustibili distinti.

Contents

List of Figures

List of Tables

List of Acronyms

A/F	Air/Fuel ratio
ANN	Artificial Neural Network
ASIC	Application Specific Integrated Circuits
BSFC	Brake-specific fuel consumption
CAaTDC	Crank Angle after Top Dead Center
CN	Cetane Number
CNL	Combustion Noise Level
CO	Carbon Monoxide
DoE	Design of experiment
DPF	Diesel Particulate Filter
ECU	Engine Control Unit
EGR	Exhaust Gar Recirculation
FAME	Fatty Acid Methyl Esters
FPGA	Field Programmable Gate Array
HC	Hydrocarbons
HHV	Higher Heating Value
HRR	Heat Release Rate
ID	Ignition Delay
IMEP	Indicated Mean Effective Pressure
LHV	Lower Heating Value
NIR	Near Infrared fuel sensor
NO_x	NO and NO_2 (combined)
NVH	Noise Vibration and Harshness
OME	Oxymethylene dimethyl ether
PID	Proportional–Integral–Derivative controller
SF	Sensitivity Factor
SOC	Start Of Combustion
SOI	Start Of Injection
TAC	Total Aromatic Content
X10	Position of 10% of fuel mass burned
X50	Position of 50% of fuel mass burned

1 Introduction

1.1 Motivation

The diesel engine is considered one of the most efficient thermal machines. Its efficiency is mainly based on fuel consumption. Although it has many advantages over other engines, it has some disadvantages. One of these is the exhaust gas content. In fact, the biggest problem with diesel engines is that the exhaust gas contains more toxic elements for health and the environment. That is why, in the recent years global emissions standards have become more and more stringent when we refer to diesel engines.

Lawmakers around the world continually restrict the already strict emission limits that exist, due to concerns over global warming caused by greenhouse gas emissions and health impacts from a variety of emissions from internal combustion engines. Current concerns over global warming and the dependency on crude oil have the lawmakers around the world establishing strict fuel economy requirements, along with imposing more strict emissions limits. Those limitations have prompted manufacturers to develop new strategies to address the challenges presented by the latest fuel economy standards and emissions regulations. The end result is a constant search for new strategies and technologies for internal combustion engines that increase efficiency while reducing emissions.

In order to achieve the emission or efficiency targets it is necessary to control the combustion behaviour. This is possible with closed loop combustion control, where the signal of the cylinder pressure sensor is used to control the combustion phasing. In parallel, research into alternative fuels has been carried out which could lead to better efficiency and lower emissions. Moreover, engine design could be implemented in several countries or even across the continent. However, there could be extreme fuel variation in different countries that could lead to a deterioration in emissions. Therefore, fuel identification becomes important in order to send the information to the ECU for calibration optimization.

One of the proposed approaches to identify the fuel is to use the fuel sensor to return one or more fuel properties. However, this has not been established and is still in a research and study phase. Another promising approach, which is discussed in this work, could be to identify the fuel through closed loop combustion control and therefore through the analysis of the combustion characteristics derived from the cylinder pressure sensor.

1.2 Scope of the work

This research study has the main goal of identifying the fuel that runs in the engine by using in-cylinder pressure sensor, with which it would be possible to optimize the combustion process. This allows the ECU to be supplied with information so that the combustion strategy can be changed according to the fuel in use, in order to achieve greater efficiency and lower pollutant emissions. At the beginning of this work, few studies were carried out on the possibility of identifying the fuel by combustion characteristics. Researches are focused on the use of an additional fuel detection sensor. The desire to figure out how changes in the fuel influenced the combustion process and the resulting emissions motivated this work. As the implementation of these strategies in future vehicles is highly likely, understanding the difficulty and robustness of using the in-cylinder pressure sensor is of great benefit.

Therefore, the work objectives are:

- To identify the robust combustion characteristic that correlate with fuel property
- To use the identified combustion characteristic and develop an algorithm to predict the fuel in use

1.3 Thesis Outline

The relevant properties of fuels are discussed in chapter 2 and their influences on combustion characteristics are evaluated. Furthermore, the state of the art for fuel identification via hardware and software was analyzed.

Chapter 3 presents the identification of the combustion characteristic suitable for identifying the fuel property and the development of the algorithm.

The validation of the function is presented in the following chapter by simulating cylinder pressure sensor drift and pressure signal noise.

2 State of the art

In order to identify the fuel by combustion characteristics, it is essential to understand the combustion behaviour. First of all in chapter 2.1 the ECU and combustion control strategies through open and closed loop control are described. In chapter 2.2 relevant fuel parameters for control are described and in the following chapter their influence on combustion with a literature-based overview. Furthermore, in chapter 2.4 an overview of the state of art on fuel identification via hardware and software is given.

2.1 ECU control strategy

In order to provide flexibility on injection schemes mainly to achieve the lowest emission targets, diesel engines are controlled by the Engine Control Unit (ECU). The evolution of the ECU over the years has been motivated by emission control and has benefited from the ever-increasing electronic capabilities.

Already in the 1970s the first progress of the ECU was made in Ford, Hagen [1] and Brietzman [2]. While at Bosch, Gerhardt [3] reports that electronic systems began with a simple injection system with a separate ignition unit in the early 1970s, and then injection and ignition were integrated into a single electronic control unit in the 1980s. Look-up tables were and are still widely used in engine management strategies to characterize nonlinear relationships between inputs and the desired output [4]. Moreover, new features such as the use of Field Programmable Gate Array (FPGA) or Application Specific Integrated Circuits (ASIC) now significantly improve the ECU's capabilities [5].

In general, the functionality of the ECU is to respond to torque and A/F requests from both internal functions (e.g. engine start, idle control, catalyst heating) and external systems (e.g. driver’s request, transmission or dynamic vehicle control). The actual torque demanded, commonly referred to as wheel torque, is required to overcome all vehicle-related driving resistances such as drag, rolling resistance or inertia forces during acceleration [6]. Considering the torque losses relative to the transmission and engine protection limitations, the gross torque indicated is obtained. The fuel path and air path shall generate strategy at the required gross specified torque considering information related to the operating point and engine condition.

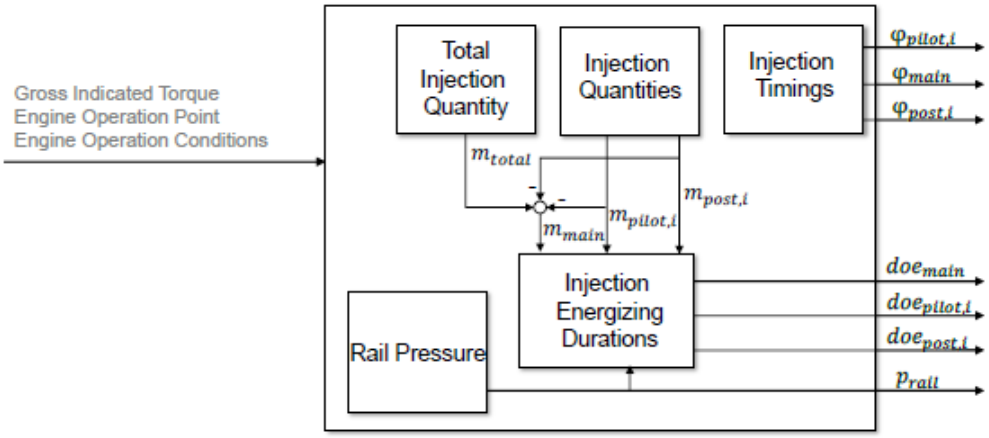

Figure 2.1: Open-loop, map-based ECU control concept according [7]

The controller provides for the application of a multi-injection strategy, in which each injection event is fully described by its injection time (φ) and energizing duration (doe). Injection quantities are calibrated rather than energizing durations due to their independence on the applied rail pressure. The corresponding energizing durations are obtained from a map of the injector, taking into account the rail pressure. Based on the gross indicated torque requirement, the total injection quantity is obtained from a conversion map. The calibration parameters for injection timing, energizing duration and rail pressure are stored in engine operation point, mode and condition dependent map structures.

In view of the engine's targets in terms of engine performance, fuel economy, pollutant emissions and NVH behavior, the calibration of the fuel path is conducted through an optimization scheme according to the design of experiment method (DoE) [8]. DoE describes a statistical approach, commonly used to identify optimal engine behaviour based on strategically chosen engine tests, mainly in steady state engine operating conditions.

In addition to the open-loop control strategy, an advanced strategy used in the ECU is the close-loop strategy. Feedforward only control approaches are generally referred to as open-loop control while control approaches that include a feedback control element are referred to as closed-loop control. The feedforward control path creates an instant control action, based on references. This allows an instantaneous control action and it is able to cover transient control actions. However, control accuracy may be limited due to model inaccuracies or unexpected behavior of the controlled system due to process disturbances.

In order to limit the impact of process disturbances on the accuracy of the feedforward control, the feedforward controller is added, if the disturbances are known a priori. The feedback controller considers information that are sent by the sensors of the controlled system, thus directly acting on

the control error by compensating for model inaccuracies or unexpected system behavior, so that the control error is as low as possible. However, typically several control cycles are required to achieve control convergence due to the delay in system information. Therefore, the combination of feedforward control and feedback provides a suitable control layout to cover both transient control capability and low control errors.

The main advantage of closed-loop combustion control over the map-based approach is a decreasing calibration effort with greater control robustness [9]. Common closed-loop approaches are based on the PID controller [10], which attempts to minimize the control error (e) by adjusting the actuation variable (u) according to equation 2.1

$$u(t) = K_P e(t) + K_I \int_0^t e(t)dt + K_D \frac{de(t)}{dt} \qquad (2.1)$$

The control parameters (K_P, K_I, K_D) are the adjustable coefficients of proportional, integral and derivative terms. The proportional term considers the present control error, the integral term considers the history of the control error behavior and the derivative term considers possible future trends considering the control error gradient. However, the derivative term is commonly ignored in combustion control related applications due to its high sensitivity to sensor measurement noise.

For this purpose, several combustion control sub-modules can be assembled in parallel to create a complete control architecture, as shown schematically in Figure 2.2.

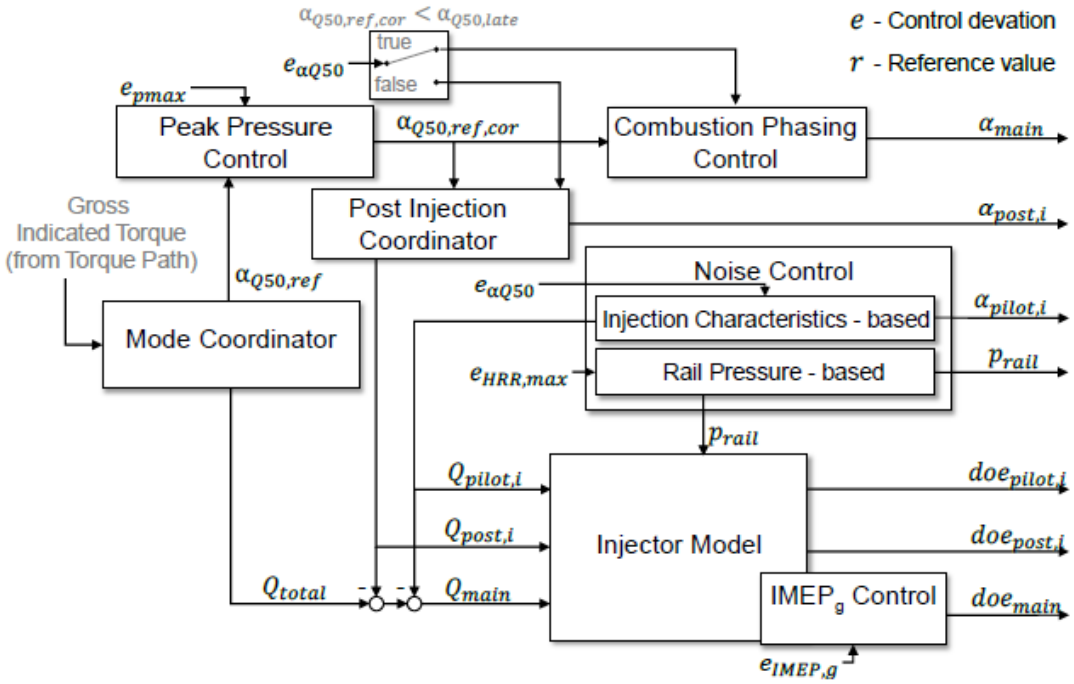

Figure 2.2: Closed-loop control approaches according to [11]

The mode coordinator generates a combination of total heat and combustion phasing, based on the requested gross indicated torque. This is based on the physical idea that an individual combination of total heat and combustion efficiency results in a corresponding combination of indicated gross average pressure and exhaust gas enthalpy [11].

In order to prevent violations of peak pressure limits, the reference value of the combustion phase, which comes from the mode coordinator, is further corrected by the peak pressure controller. The combustion phasing controller finally adjusts the timing of the main injection to obtain the correct combustion timing reference value. Peak pressure control and combustion phase control are both performed by the I-controller.

The combustion noise controller is divided into two sub-modules, a rail pressure-based control part and an injection characteristic-based control part. The rail pressure level is important to ensure sufficient air-fuel mixture preparation quality and thus limit soot emissions. But since high rail pressures can compromise the combustion sound level, the pilot injection characteristic is chosen as an additional degree of freedom to find an appropriate compromise between combustion sound level and soot emissions. The rail pressure-based control is realized by PI control and controls the peak heat release rate since it affects combustion noise. The pilot injection characteristics-based control part controls the combustion noise level via a state machine, which chooses the right pattern of pre-calibrated pilot injection events. Since pilot injections generally compromise soot emissions, the state machine avoids its activation wherever the reference combustion noise limit is not exceeded.

The post-injection coordinator comes into play when the reference values of the late combustion phase ($\alpha_{Q50,\ Ref,\ cor} > \alpha_{Q50,\ late}$) are requested by the mode coordinator to start the heating or regeneration modes. The implementation of very late combustion phases with the delay of the main injection event only can lead to disadvantages related to combustion stability and oil dilution [12]. To avoid these problems, additional post-injection events are added to the injection model.

Once the fuel injection energies for the pilot, main and post-injection events are obtained, they are transferred to the corresponding excitation durations via the injector map considering also the rail pressure. Since many sub-models are involved, from the definition of the mode coordinator reference point to the injector model, a resulting deviation of the control in the indicated mean gross effective pressure can be expected. To eliminate these remaining control deviations, an additional I-controller is provided, which only acts on the excitation duration of the main injection event [11].

Summarising the closed-loop combustion control architecture presented, it can be seen that all important combustion characteristics are captured through the given approach. But a disadvantage of this concept is that each combustion characteristic is controlled independently by the individual controllers, resulting in a cascade control architecture

2.2 Relevant parameters of the fuels for control

Fuels are compounds with stored potential energy, which through combustion can be released and transformed into different types of mechanical energy. Although they can be found in all three states (liquid, gaseous and solid), the most used in vehicles are liquid fuels. Some of the advantages of liquid fuels are that they can be easy to handle, transport and can take the form of any type of container. In order to perform fuel quality analysis, it is important to figure out what properties define a good quality fuel. In this regard, a review of previous work on this topic has been carried out and the results are shown in this chapter. It is generally recognized that fuels have a number of classification parameters. Many of them are also mentioned in standards (e.g. EN590, ASTM 975) and legislated. However, only some of the parameters are described in this chapter. Those are mostly representative for measuring fuel quality by combustion characteristics. Each of these parameters can be taken and analysed independently.

Property	**Unit**	**Lower limit**	**Upper limit**	**Test Method**
Cetane number	-	51.0		EN ISO 5165
Cetane index	-	46.0		EN ISO 4264
Density @ 15°C	kg/m^3	820	845	EN ISO 3675, EN ISO 12185
Viscosity at 40°C	mm^2/s	2.0	4.5	EN ISO 3104
Sulphur content	mg/kg		10.0	EN ISO 20846, EN ISO 20847
Flash point	°C	55		EN ISO 2719
Carbon residue	% m/m		0.30	EN ISO 10370
Ash content	% m/m		0.01	EN ISO 6245
Water content	mg/kg		200	EN ISO 12937
Total contamination	mg/kg		24	EN ISO 12662
Fatty Acid Methyl Ester (FAME) (biodiesel) content	% v/v		7	EN 14078
Polycyclic aromatic hydrocarbons	% m/m		11 (8)	EN ISO 12916

Table 2.1: EN590 requirements and test methods [13]

Cetane Number

The cetane number is a measure of how readily the fuel starts to burn (auto ignites) under typical conditions verified in a diesel engine combustion chamber. A fuel with a high cetane number starts to burn shortly after it is injected into the cylinder; therefore, it has a short ignition delay period. Conversely, a fuel with a low cetane number resists autoignition and has a longer ignition delay period. [14]Other effects of cetane number on engine performance result in increased engine noise with lower cetane number.

Heating Value

The heating value of fuel can be defined in two ways: the higher heating value (HHV), or gross calorific value, and the lower heating value (LHV), or net calorific value. HHV is determined by bringing all the products of combustion back to the original pre-combustion temperature, and in particular condensing any vapour produced to liquid water, while LHV is based on gaseous water (steam) and is determined by subtracting the heat of water vaporisation from the HHV [15]. Although HHV has a wider acceptance in biomass characterization (biomass is renewable energy from plant sources), engine performance estimation models usually use LHV of the fuel. This is due to the fact that automotive fuels contain only a small amount of water (<0.05% by mass) that can be neglected when estimating the heating value [16]

Density

Density is also an important fuel parameter that defines its quality. Density defines in a way, fuel economy and maximum power. It describes the amount of energy per unit volume. It is a very important factor because fuels are purchased in volume. Low density fuels will have better spray dispersion and penetration. But these factors cannot be positive for all types of engines as what can be positive for one type of engine configuration (combustion chamber geometry, compression ratio, turbulence type, air/fuel ratio, etc.) can be detrimental to other types. Therefore, influences on fuel density still need to take into account engine operating points, injection pressure, injector type or combustion chamber geometry to confirm its influence on emissions or engine performance. However, density is one of the best characteristics to determine a particular fuel type and its knowledge can have a positive impact on the engine's operating strategy [17].

Viscosity

Viscosity is an important parameter for fuels as it indicates the resistance of the fuel to flow. This means that if the fuel has a low viscosity, the fuel injection system may be subject to high temperatures with an increased risk of cavitation wear and erosion. In addition, low viscosity fuels

are also more likely to leak. Higher viscosity fuels (e.g. B100) require higher injection pressure. In addition, highly viscous fuels would result in the formation of larger droplets and therefore the type of spray may change [17].

Total Aromatic Content (TAC)

TAC represents the total numbers of C/H ratios present in the fuel, compounds with at least one or two benzene like ring structures. Aromatics are chemically defined as the class of compounds derived from benzene (C_6H_6) that contain a closed ring of six carbon atoms. The term "aromatic" also applies to other ring compounds, often containing hetero-atoms, which have a fully conjugated double bond system. Aromatic compounds may also have more than one ring in their structure and may have aliphatic chains or rings attached to one or more of the base rings [18]. The latter category is of great importance when the aromatic content of diesel is considered.

FAME content

Fatty acid methyl esters (FAME) are the result of alkali-catalysis between fatty acids and methanol. The physical characteristics of fatty acid esters are closer to those of fossil diesel fuels than pure vegetable oils, but properties depend on the type of vegetable oil. A mixture of different fatty acid methyl esters is commonly referred to as biodiesel, which is a renewable alternative fuel. FAME has physical properties similar to those of conventional diesel. It is also non-toxic and biodegradable [19].

Oxygen content

The addition of biomass in the new diesel blends has also led to the oxygen content being considered as an important parameter to identify the fuel. In some blends the oxygen content exceeds 20%, which can affect not only other properties such as cetane number or heating value, but also directly some combustion characteristics such as ignition delay, heat release value and the cyclic variation of parameters [20].

The most important fuel parameters have been presented with regard to their influence on combustion. When fuel qualities are easy and fast to detect, they could be used to adapt the engine operating strategy in order to optimize combustion. It has to be said that fuels are characterised by many other parameters that have not been discussed in this document, such as sulphur content, ash content, water content, corrosivity total contamination, etc. But they are not easy to detect and analyse and to correlate them with combustion behaviour and, therefore, have not been presented.

2.3 Influence of the fuel properties on combustion characteristics

Numerous studies have been conducted to clarify the relationship between the properties of diesel fuel and combustion behaviour. Many of these studies have been conducted using real engines with steady-state cycle or transient mode operation.

Yoshiyuki et al. in their research [21] claim that when cetane number decreases, ignition delay becomes long. As shown in the Figure 1, ignition delay maintains the same trend at both high load (a) and low load (b), with other boundary conditions constant. While the other characteristics, such as maximum cylinder pressure p_{max}, maximum pressure gradient $dp/d\theta_{max}$, maximum heat release rate $dQ/d\theta_{max}$, ignition delay τ, the rate of heat release in premixed combustion stage to total heat release Q_{pre}/Q_{total} and combustion duration $\Delta\theta_{burn}$, have a different behaviour in the two engine operation point

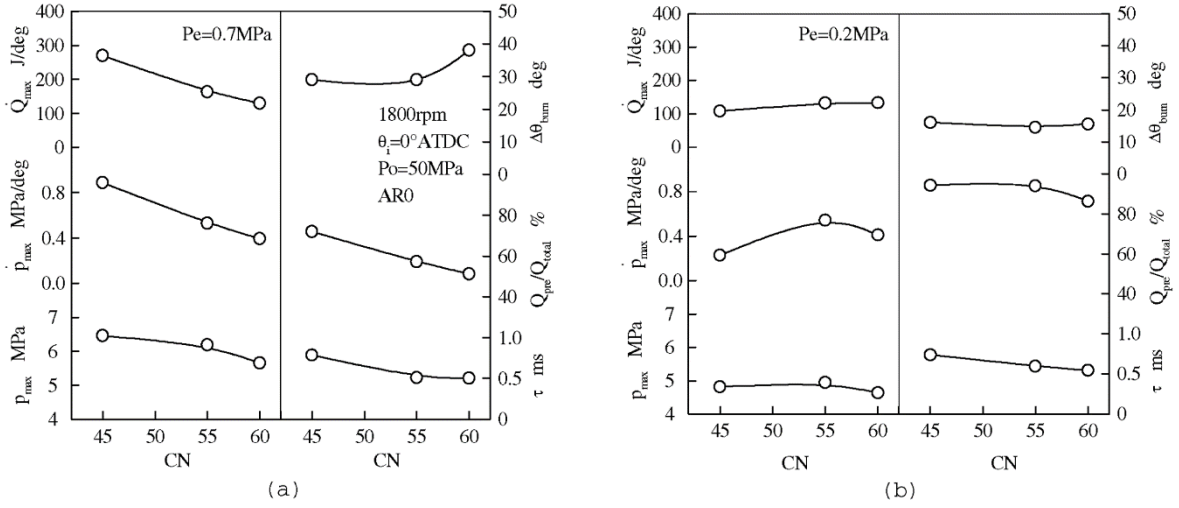

Figure 2.3: Effect of cetane number on combustion characteristics [21]

This is because, according to Yoshiyuki et al., at low load conditions at low temperature, low cetane fuel forms a fuel-air mixture that is leaner than the fuel limit due to a long ignition delay.

Another study of Koehler et al. [22] confirms this statement. They claim that low cetane fuels have a higher ignition delay and stronger pre-mixed combustion. They also have a short combustion phase duration at limited speed. As the cetane number increases, the ignition delay is reduced together with the duration of the premixed combustion phase, thus increasing the duration of the limited speed combustion phase (Figure 2).

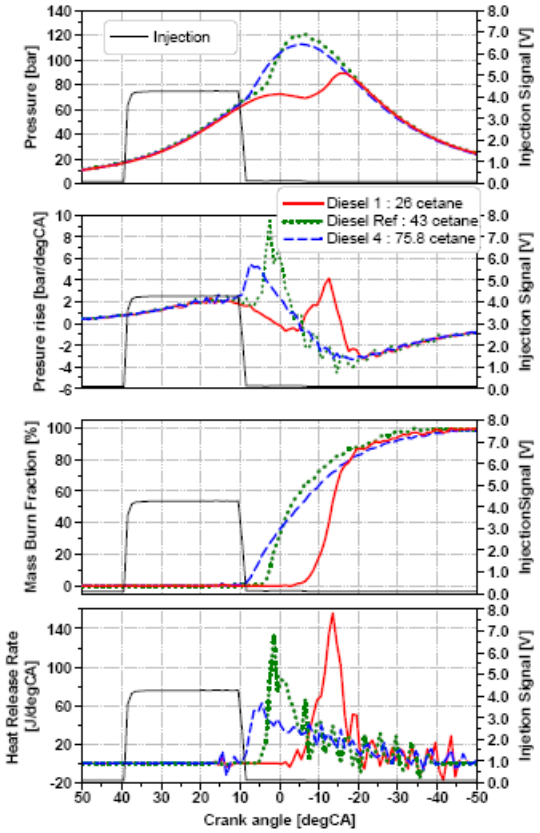

Figure 2.4: Combustion analysis for three fuels [22]

In other studies, the influence of cetane number on combustion quality and engine performance is unclear, and results are divergent due to different test conditions. For example, Rose et al. [10] claim that a low cetane number increases the noise of diesel engines with high part load, while De Ojeda et al. [6] claim that a low cetane number leads to truly unstable engine operation at low load conditions, but this cannot be fully attributed to the cetane number alone. In conclusion, it could be said that there are many other factors that influence combustion quality and emissions and that cetane number has a significant impact on the ignition delay factor. Factors such as the operating speed, the fuel types used in the test process and the engine configuration are the ones that distinguish each test. However, knowing cetane number, the engine operating strategy can be adapted for maximum engine efficiency.

The effects of the oxygen content are not as sharp as those seen with the cetane number, this is because it is not easy to isolate the oxygen content as the only variable to be modified. A modification of the same goes to affect other parameters such as heating value and viscosity.

Haiwen et al. in their article [23] claim that by increasing the oxygen content the ignition delay is shorter. However, it is not possible to state precisely that the reduction of the ignition delay is an exclusive cause of the increase in oxygen content, since, as can be seen from the Figure 3, it even

reduces with the increase in cetane number, confirming what has been argued in the studies previously illustrated.

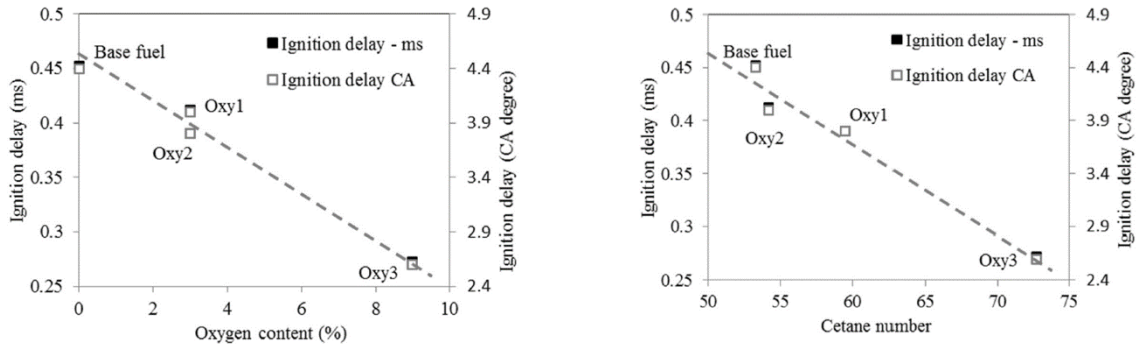

Figure 2.5: Influence of oxygen content and cetane number on ignition delay [23]

Labeckas et al. [20] in their work analyse the combustion behaviour by blending diesel with ethanol or biodiesel and assert that the ignition delay does not show a clear trend with increasing ethanol(Figure 4a) or biodiesel (Figure 4b) content.

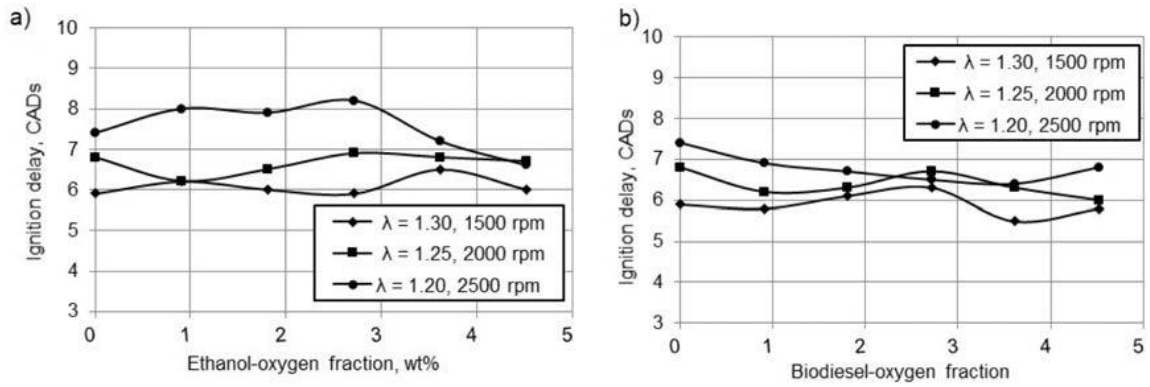

Figure 2.6: Influence of ethanol-oxygen and biodiesel-oxygen fraction on ignition delay [20]

Similarly, they claim that maximum heat release rate does not show a clear correlation with oxygen content. They also point out that the oxygen content does not greatly affect the burn angle X50 and thus the performance efficiency of an engine. Regarding the end of X90 combustion was concerned, they found divergent behaviour if diesel was mixed with ethanol or biodiesel. With the addition of ethanol, the combustion ends earlier, while with the addition of biodiesel it ends later. In addition, the maximum pressure peak was also analysed, which increases with the increase in oxygenated fuel.

The effects of the aromatic content are studied by Yoshiyuki et al. [21]. They investigated three fuels with the same cetane number and different aromatic content of 0%, 24% and 38%. Combustion characteristics were analyzed such as maximum cylinder pressure p_{max}, maximum

pressure gradient $dp/d\theta_{max}$, maximum heat release rate $dQ/d\theta_{max}$, ignition delay τ, the rate of heat release in premixed combustion stage to total heat release Q_{pre}/Q_{total} and combustion duration $\Delta\theta_{burn}$.

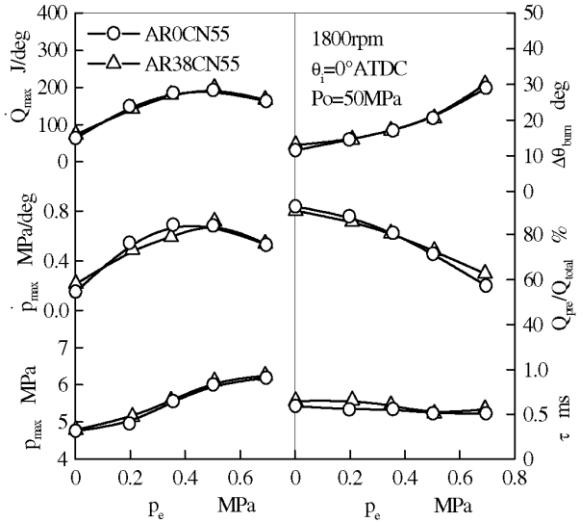

Figure 2.7: Influence of aromatic content on combustion characteristics [21]

As can be seen from the Figure 5, the aromatic content does not directly affect the overall combustion characteristics, maintaining the same cetane number.

The common finding from literary research is the direct correlation of cetane number on ignition delay: an increase in cetane number reduces the ignition delay. A smaller influence of oxygen content was found. However, a change in oxygen content causes a change in other properties, so the impact of the oxygen content on combustion cannot be defined independently.

2.4 Identification of the fuel properties via hardware and software

As already mentioned, work and research has been spent in recent years on private research companies or vehicle manufacturers to bring their engine emissions into line with stricter emissions legislation. One way developed by manufacturers is to use alternative fuels to reduce polluting emissions, given the continuous spread of natural fuels and biodiesel that allow less environmental pollution. However, these fuels used in parallel with diesel have different properties and, consequently, the combustion and behaviour of the engine is different. It becomes therefore fundamental to identify the fuel that runs in the engine in order to return the correct information to the ECU and to modify the calibration of the engine to obtain a higher efficiency and lower pollutant emissions.

To detect the fuel and its properties, manufacturers have developed both hardware and software technologies. In this chapter most important developed strategies are described and how these are applicable in vehicles.

2.4.1 Onboard technologies for fuel quality measurement

One way to identify the fuel is to use onboard hardware technologies, reproducing laboratory systems. With these technologies it is possible to identify one or more properties of many fuels. The main problem is the reaction time required when these are installed onboard. In fact, these systems must provide similar qualitative and quantitative responses compared to laboratory systems but with a greater speed.

One technology used is the tuning fork, which is an acoustic resonator in the form of a two-pronged fork with the prongs formed by a U-shaped bar of elastic metal. In order to resonate when excited, the two peaks of the fork are metallic. If, for example, sinusoidal tension is applied in air or vacuum, the thin metal film on the quartz fork will bend due to mechanical stress. It must be said that the use of a piezoelectric substrate allows the mechanical excitation of the tuning fork to be replaced by an electrical excitation. If the fork is immersed in a liquid environment (e.g. fuel, oil, water, etc.), a change in the oscillation frequency can be observed (Figure 6) due to the characteristics of the medium (e.g. viscosity, density) and the friction of the fork with the medium [17].

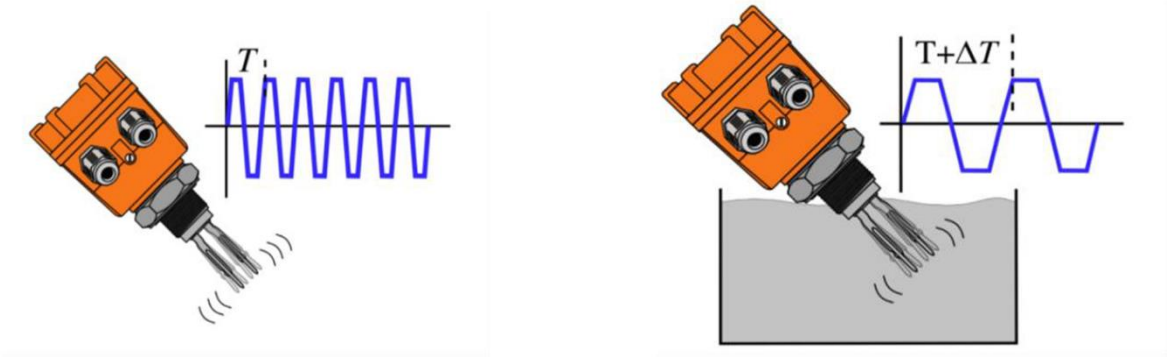

Figure 2.8: Tuning fork frequency in air (input) (left) and tuning fork frequency in liquid (output) (right)

Using an algorithm for the interpretation of the measured signals, together with a database of fluid characteristics, a sensor equipped with a similar tuning fork is able to measure different viscosities, fluid densities and their dielectric constant and depending on these values fluids can be identified.

The advantages of this technology are the accuracy and repeatability of its measurements [24]. Furthermore, they are small, compact and robust without moving parts. The advantage of this sensor is that it can be mounted in almost any position, in line or in the tank. Temperature and fluid are also not relevant for operating a tuning fork sensor [24]. Another advantage is the number of

measured parameters. As already mentioned, the sensors can measure up to four fluid properties: viscosity, density, dielectric constant and fluid temperature. In addition, combinations of dielectric constants and density, for example, can offer other information such as the concentration of one fluid type in another.

One of the disadvantages is that the sensor fork may be subject to material accumulation, which may cause inaccuracies in the readings. A second disadvantage would be that other fuel parameters cannot be read. Important parameters for combustion optimization such as cetane index or aromatic content are not detected.

In addition to the tuning fork, another technology developed in recent years is near infrared (NIR) spectroscopy technology. NIR spectroscopy is considered an analytical technique. It is based on the absorption of electromagnetic radiation having wavelengths in the region of about 750 - 2500 nm. The molecular construction consisting of atoms is in constant vibration and if a light source is used to send a type of photonic energy at a certain wavelength, the amplitude of the vibration will change. The remaining photon flux continues to propagate until a NIR detector detects it.

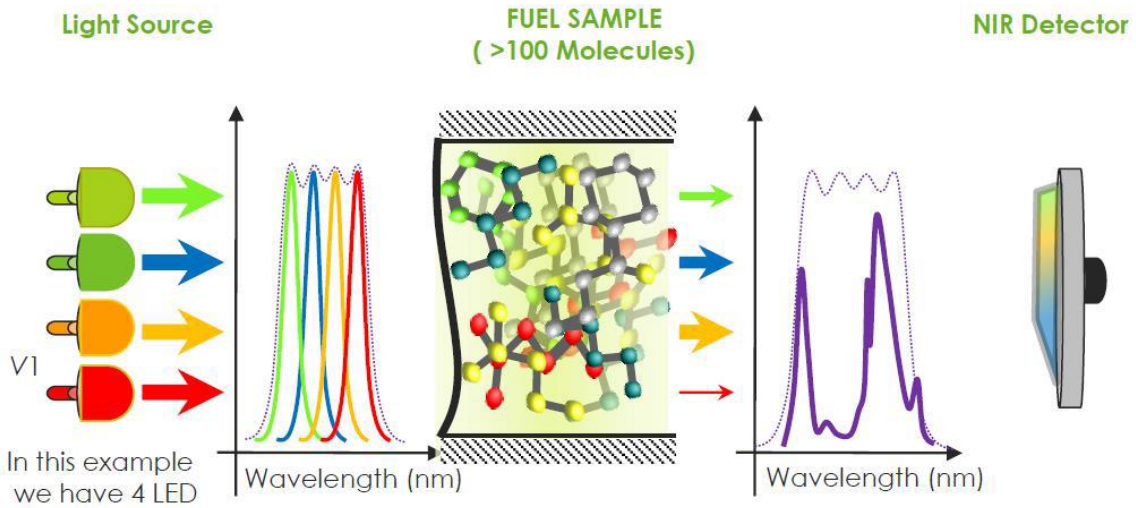

Figure 2.9: NIR spectroscopy functioning principle

By comparing the light emitted at a certain wavelength with that detected, the NIR absorption spectrum can be drawn (Figure 7). This is considered to be the operating principle of NIR spectroscopy. By analyzing the spectrum read by NIR it is possible to derive the molecular structure and consequently to obtain the properties of the fuel.

Among the advantages of this technology the most important one is that it is a non-invasive / non-destructive technique. It is a fairly complex technique capable of determining both the physical properties of the fluid (e.g. Density, viscosity) and the chemical properties (e.g. Aromatic content,

oxygen content, etc.). Depending on the capacity of the decoding algorithms, these sensors are able to read from six to fifteen parameters (e.g. density, bio content, aroma content, fuel type, cetane number, etc.). On the other hand, the limited wavelength range may be the most important disadvantage, with difficulties in interpreting highly absorbent samples. In these cases, small variations in ppm concentrations may not be detected [25] [26].

2.4.2 Fuel properties prediction via software

Another way to detect fuel properties is to develop algorithms that can predict them. The most important advantage of using a fuel property prediction model is that it reduces the complexity of the hardware to be installed as well as reducing costs. On the other hand, it increases computational complexity and computational effort. So, these strategies offer a considerable advantage but the research work is mainly aimed at reducing the required computing capacity so that it can be installed onboard.

Solomon et al. [27] have used mathematical models, statistical models and artificial neural network (ANN) to predicting the properties of biodiesel. The ANN method involves the use of certain properties of biodiesel that have been previously known or obtained through experimental results to predict other fuel properties. With their work, they claim to detect the cetane number and density of the fuels under examination with high accuracy (Figure 8).

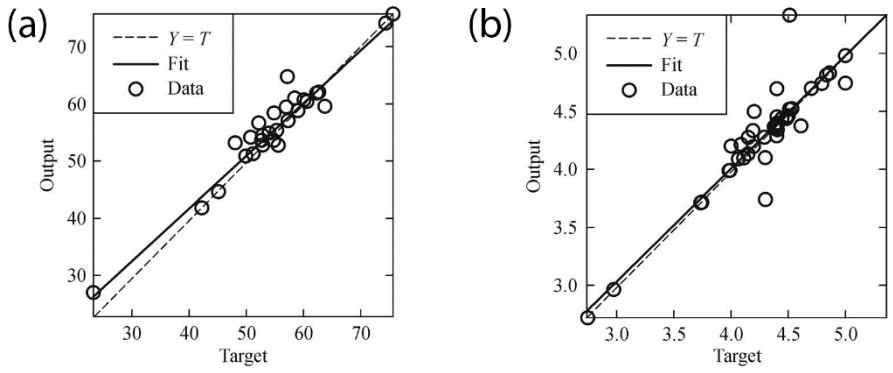

Figure 2.10: Regression plot for Cetane Number(a) and density (b), [27]

Cheenkachorn [28] using the data mainly collected from previous literatures, statistical models and artificial neuron networks (ANN), asserts that it detects the properties of the fuel, such as viscosity and Higher Heating Value (HHV) number, with high accuracy.

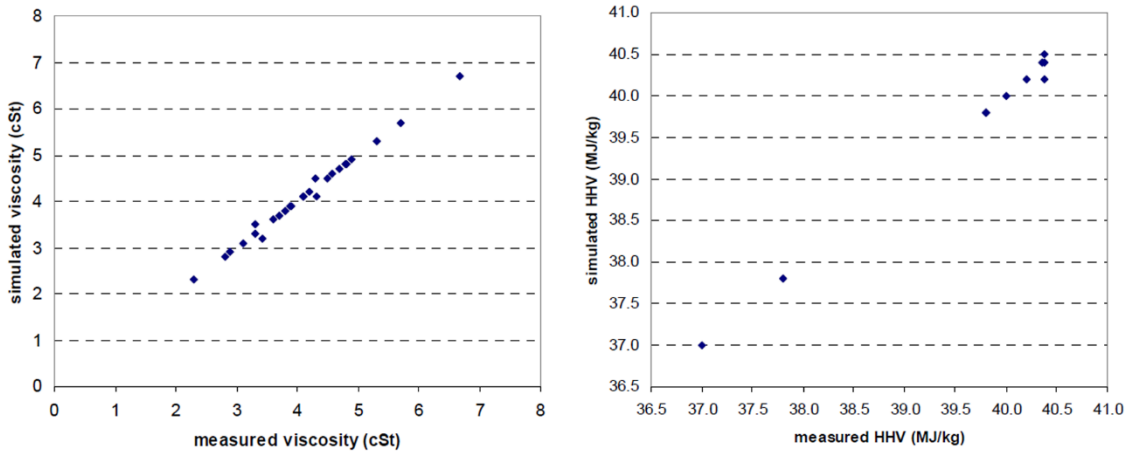

Figure 2.11: Viscosity and Higher Heating Value prediction [28]

Other studies have been made to identify fuel characteristics. All these studies, however, are difficult to apply onboard, for online fuel detection. This is due to the considerable calculation capacity required. Another aspect for which these strategies have not yet been developed onboard is that they are not able to detect fuel properties with technologies already installed on vehicles, but require the installation of new hardware in order to detect other characteristics.

2.5 Summary and conclusion

It has been seen as there are several ways to identify the fuel on board. The solution that is currently at the most advanced stage of research but not yet in series application is the use of the fuel sensor, which however requires an increase in hardware complexity on board. Alternative solutions of software-based calculation models have been studied, but in this case the main problem is the computational effort required in fuel quality prediction. Therefore, in this work an alternative method for fuel identification has been developed, using the hardware already in use in series applications, such as the cylinder pressure sensor, with which the combustion characteristics can be calculated with a closed loop control and the relative fuel derived.

3 Fuel identification algorithm based on cylinder pressure sensor

As described above, it is possible to detect fuel qualities through fuel quality sensors, which are able to detect certain characteristic properties of the fuel. However, this approach is still in the research phase and not yet applied in series. Moreover, this involves the additional installation of these technologies, which are still too expensive for series applications.

The main challenge of this work is to be able to identify the fuel through the technologies already present on vehicles, and in particular using the in-cylinder pressure sensor. In fact, with this sensor it is possible to derive the combustion characteristics and from the different combustion process to identify the different fuel in use.

In this chapter combustion characteristics useful for the purpose of the work are described, then the effects that the different fuels cause on combustion are analyzed and the correlations between the properties of the fuels and the combustion characteristics are highlighted.

An additional analysis and simulation have been made on the possibility of the pressure sensor drift and pressure signal noise and the consequences on the combustion characteristics.

3.1 Combustion characteristics for fuel detection

Combustion can be associated with specific characteristics of the combustion process, which can be used for targeted handling and optimisation of engine behaviour. An overview of the combustion characteristics useful for the description of the combustion process is made. After that, experiments directly on the engine are carried out in order to analyze the combustion process for three different fuels. This analysis will then be validated with a second experiment carried out on a single-cylinder research engine.

3.1.1 Combustion characteristics overview

An overview on available combustion characteristics is given in Figure 3.1.

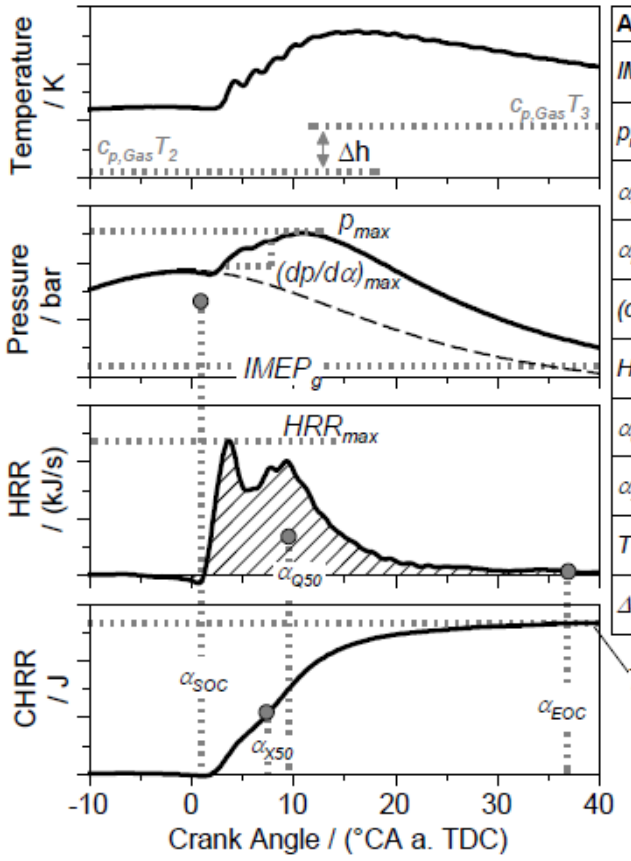

Abbrev.	Unit	Description
$IMEP_g$	bar	Gross Indicated Mean Effective Pressure
p_{max}	bar	Peak Cylinder Pressure
α_{SOC}	°CA a TDC	Crank Angle Position of Start of Combustion
α_{EOC}	°CA a TDC	Crank Angle Position of End of Combustion
$(dp/d\alpha)_{max}$	bar/°CA	Peak Cylinder Pressure Gradient
HRR_{max}	kJ/s	Peak Heat Release Rate
α_{q50}	°CA a TDC	Crank Angle Position of Centroid of Combustion
α_{x50}	°CA a TDC	Crank Angle Position of 50% Mass Fraction Burnt
TCHRR	J	Total Cumulated Heat Release Rate
Δh	J/kg	Specific Enthalpy Difference

Figure 3.1: Overview of combustion characteristics [11]

The average gross pressure indicated ($IMEP_g$) is an indicator of a motor's ability to produce torque. It is calculated during the compression and expansion phase of the high-pressure cycle, with the ring integral of the cylinder pressure trace, equation 3.1.

$$IMEP_g = \frac{1}{V_h} \oint p \, dV \qquad (3.1)$$

The indicated gross efficiency ($\eta_{i,g}$) of the combustion process is given by equation 3.2, taking into account the lower heating value (LHV) and the total amount of fuel (m_{fuel})

$$\eta_{i,g} = \frac{IMEP_g \, V_h}{m_{fuel} \, LHV} \qquad (3.2)$$

The total cumulative heat release rate ($TCHRR$) represents the total energy which is converted during the combustion process into pressure work and wall heat loss according to equation 3.3.

$$HRR = \frac{k}{k-1} \, pdV + \frac{1}{k-1} \, Vdp + \alpha_w A_w (T - T_w) dt \qquad (3.3)$$

The first term considers the change in the volume of the combustion chamber (dV) by the movement of the piston. Due to the inertia of the mechanical components, mechanical energy is stored in the system during the expansion phase. During the compression phase in turn, this

mechanical energy is returned for gas compression. The second term takes into account the change in gas pressure (dp) as a result of gas compression, gas expansion and combustion. Combustion causes an increase in gas pressure, generating a corresponding gas force on the piston from which torque is obtained at the crankshaft. The heat losses of the combustion chamber walls are determined by the temperature difference between the working gas (T) and the combustion chamber walls(T_w). The extent of heat transfer to the wall is significantly influenced by the heat transfer coefficient to the wall(α_w).

An indicator of the gross efficiency indicated is the combustion phase. There are two definitions of combustion phases used in the literature. First, the position of the crank angle, where 50% of the total amount of fuel is burned (α_{x50}). However, this definition has disadvantages when considering combustion strategies with the presence of post injections, such as exhaust gas heating or regeneration strategies. A second definition has been introduced to take late combustion events into account in view of their influence on the gross efficiency indicated. The combustion centroid (α_{Q50}) is defined as the centroid of the area enclosed by the heat release rate profile between the start of combustion of the position (α_{SOC}) and the end of combustion (α_{EOC}), equation 3.4

$$\alpha_{q50} = \frac{\int_{\alpha_{EOC}}^{\alpha_{SOC}} \alpha \, HRR \, d\alpha}{\int_{\alpha_{EOC}}^{\alpha_{SOC}} \alpha \, d\alpha} \qquad (3.4)$$

The crank angle position at the start of combustion (α_{SOC}) defines where combustion begins. It is defined as the point at which the measured pressure profile begins to deviate significantly from the unburned pressure profile. The start of combustion influences the combustion phase, e.g. a delayed start of combustion also causes a delayed combustion phase.

Peak pressure ($pmax$) is an important boundary condition for engine design, as it defines its full load capacity. To prevent damage to the motor, the peak pressure must be limited. But an increase in the peak pressure results in better indicated gross efficiency and thus higher power output at full load. Consequently, a compromise must be found between the mechanical strength of the engine and the permitted peak pressure. However, the total peak pressure capacity of an engine is generally not used due to the mandatory fulfilment of an engineering margin. An engineering margin is generally considered to take account of undesired fluctuations in peak pressure due to unpredictable influences on engine operation.

Combustion noise is an important parameter that influences the NVH (Noise, Vibration, Harshness) behaviour of the vehicle. Combustion noise can be divided into direct combustion noise and indirect combustion noise. Direct combustion noise is caused by combustion, which causes vibration of the chamber walls and transfers the noise outside. Indirect combustion noise results from the relative

movements of mechanical components such as cranks or auxiliary elements, e.g. the high-pressure fuel pump. The share of direct combustion noise is generally the dominant one and can be quantified by the combustion noise level (CNL). The direct combustion noise level can be obtained by frequency analysis of the cylinder pressure trace and is a suitable control value due to its real-time calculation scheme. An indicator of the combustion noise level is the peak pressure gradient ($(dp / d\alpha)_{max}$). Since the pressure gradient is linked to the heat release rate via equation 3.3, the peak heat release rate (HRR_{max}) in combination with its present position also has an influence on combustion noise. The position of the peak heat release velocity is closely related to the combustion phase.

The enthalpy difference (Δh) describes the energy difference between intake and discharge charge. It quantifies the amount of available exhaust gas waste energy, which determines the amount of heating of the exhaust gas. Assuming an average specific gas constant over the combustion cycle and neglecting the blow-by effects, the enthalpy difference can be approximated using equation 3.5.

$$\Delta h = m_{cyc} c_{p,gas} (T_{exhaust} - T_{intake}) \qquad (3.5)$$

A greater amount of exhaust energy from the exhaust compromises gross indicated efficiency. Consequently, the combustion phasing can be related to the enthalpy difference. The exhaust gas heating or regeneration modes in turn require a higher enthalpy difference to improve the conversion behaviour of the catalytic converter or to achieve a sufficient diesel particulate filter (DPF) regeneration temperature. In this case it is necessary to apply a later combustion phasing, which results in a higher total heat energy demand to obtain the same gross mean indicated pressure.

As the combustion phasing advanced, the peak combustion temperature generally increases. The increase in the peak combustion temperature in turn shows effects on emissions NOx. During the variation of the combustion phasing, the emission level of the engine is kept constant by adjusting the HP-EGR speed. As a consequence, a higher amount of inert gas in terms of EGR is required to keep the NOx emission level constant. Due to the increasing rate of uncooled HP-EGR, the intake manifold temperature increases, the filling efficiency deteriorates and the air-fuel equivalence ratio decreases. The increase in gas temperature of the cylinder filling causes a shorter ignition delay which results in a shorter mixing time for the gas/fuel mixture. Therefore, the presence of rich gas/fuel mixture regions is more frequent, which promotes the formation of soot and CO emissions. This effect is further amplified by the lower air-fuel equivalence ratio. HC emissions decrease slightly as the combustion phase advances. Higher combustion temperatures and pressures cause

more complete oxidation of fuel fragments and reduce the occurrence of wall quenching effects. The peak heat release rate is kept constant by rail pressure adjustments. The constant peak heat release rate in combination with an advanced combustion phase produces higher pressure gradients.

Ignition delay of a fuel, in the context of diesel engines, is the period from the time the first parcel of fuel enters the chamber to the point when the first flame is observed in the spray. Therefore, it is defined as the difference between Start of Combustion (α_{SOC}) and Start of Injection (α_{SOI})

$$ID = \alpha_{SOC} - \alpha_{SOI} \quad (3.6)$$

3.1.2 Experimental method

Engine System

The test engine used in this study is a 4-cylinder diesel engine. It is well equipped to provide detailed and accurate measurements of its behaviour. The main hardware configuration engine is presented in Table 3.1.

Engine type	4-cylinder, 4 valves
Bore	79 mm
Stroke	88.3 mm
Peak firing pressure	160 bar
Injection system	2200 bar common rail, 8-hole injector
Compression Ratio	15.5
Boosting system	Single stage HP - VGT
Charge cooling	Water-cooled
EGR paths	Cooled LP-EGR, cooled HP-EGR

Table 3.1: Basic specification of the 4-cylinder test engine

Moreover, in order to analyse the process correctly the boundary conditions such as coolant temperature, air temperature must be kept constant. They are reported in the Table 3.2

Fuel temperature	35°C
Fuel pressure	5 bar
Air temperature	25°C
Air pressure	1013 mbar
Coolant temperature	90°C

Table 3.2: Thermodynamic boundary condition 4-cylinder test engine

Cylinder pressure is measured in the engine with a Kistler piezoelectric pressure transducer. The pressure transducer was calibrated before the engine tests using a dead-weight pressure calibration at six different pressures, with each point repeated three times for consistency. Signal from the pressure transducer is further processed FEV's Indication system calculate the thermodynamic parameters. Other signals measured by data acquisition system include intake manifold pressure, intake manifold temperature, fuel injection line pressure, and injector current. Fuel injection line pressure and injector signal are monitored to provide details of actual injector and injection behavior in the absence of a needle lift sensor that would directly measure the opening and closing of the injector needle. To carry out the investigation two different engine platform were identified for robustness of the detection approach.

To best analyse the combustion process, the boundary conditions must be the same. Therefore, in order to understand the quality of combustion it is essential that the intake conditions such as pressure and temperature are kept constant. Table 3.3 shows conditions for engine operation points analized.

Engine operation point (Engine speed – BMEP)		**1000rpm - 7bar**	**1500rpm - 3bar**	**1500rpm - 10bar**	**2000rpm - 7bar**	**2500rpm - 7bar**
Intake pressure	bar	1.118	1211	1.398	1.256	1.436
Intake temperature	°C	32	41	35	35	44
O2 concentration	%	0.203	0.193	0.19	0.191	0.193
Rail pressure	bar	500	555	1121	1114	1141
Start of electric	CAaTDC	-7,67	-12,94	-13,65	-17,46	-22,56

Table 3.3: Operating condition for 4-cylinder test engine

To validate the study done with the 4-cylinder engine, a second analysis was carried out on a single-cylinder research engine. However, for the purpose of this work the tests can be useful in order to obtain confirmation of the study carried out. The main hardware configurations are presented in Table 3.4.

Engine type	Single cylinder, 4 valves
Displacement	390 cm3
Bore	79 mm
Stroke	88.3 mm
Peak firing pressure	160 bar
Injection system	2500 bar common rail, 9-hole injector
Compression Ratio	14
Boosting system	2-stage, HP turbine: waste gate, LP turbine: VNT
Charge cooling	Water-cooled
EGR paths	Cooled LP-EGR, cooled HP-EGR

Table 3.4: Basic specification of the single cylinder research engine

Again, the boundary conditions must be the same. Therefore, intake temperature, intake pressure, intake oxygen concentration, rail pressure and start of electric injection have been kept constant. In the table 3.5 are reported boundary conditions for single cylinder research engine.

Engine operation point (Engine speed – BMEP)		**1500rpm - 7bar**
Intake pressure	bar	0.99
Intake temperature	°C	26
O2 concentration	%	15,6
Rail pressure	bar	912
Start of electric	CAaTDC	-16,03
Fuel temperature	°C	25
Fuel pressure	bar	5
Air temperature	°C	25
Air pressure	mbar	1013
Coolant temperature	°C	90

Table 3.5: Operating condition for single cylinder research engine

Having established the test engine platforms, it was necessary to have variation in fuel to build robust model.

Test fuels

A set of three test fuels is used for 4-cylinder test engine: a common commercial diesel fuel plus two advanced fuels. They have essentially the material structure of fossil diesel but clearly exceed the specifications of all diesel fuels previously available at filling stations. Their properties are reported in Table 3.6.

Fuel	Lower Heating Value	Density 25°C	O2 mass fraction	Cetane Number
	MJ/kg	kg/m3	%	-
Diesel	42.7	828.8	0.0076	52.8
Fuel 1	43.5	771.1	0.360	67.8
Fuel 2	43.6	766.9	0.790	68.6

Table 3.6: Fuel properties for 4-cylinder engine

These fuels have been tested for combustion behaviour with different cetane numbers and densities. As can be seen from the fuel specification table, the two advanced ones have a very high cetane number compared to standard diesel, as well as a lower density. The combustion process was then compared with standard diesel.

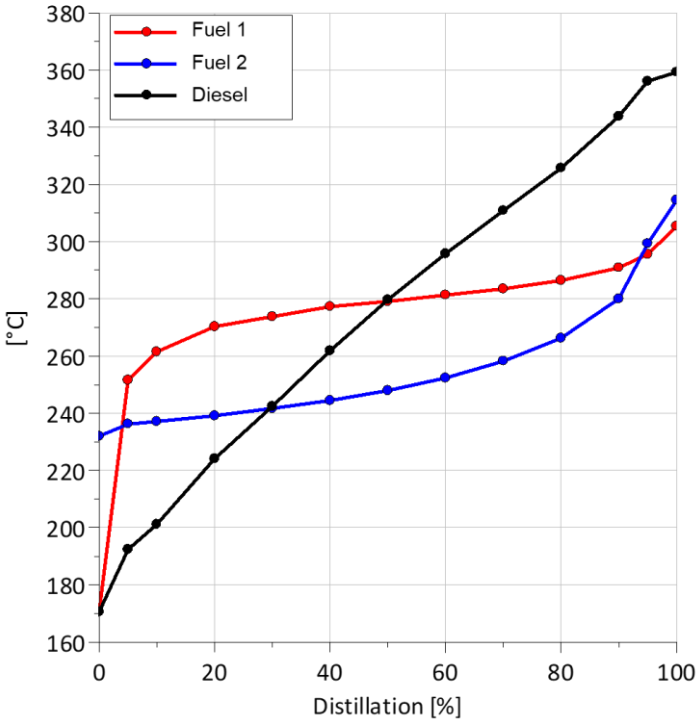

Figure 3.2: Fuel distillation curves of the 4-cylinder engine

The fuel distillation curves are also shown in the Figure 3.2. It can be seen that advanced ones require a higher temperature to start evaporating, but end their evaporation at a lower

temperature than standard diesel. This allows them a better mixture with the air in the chamber, allowing a more complete combustion with consequent advantages in terms of emissions and efficiency.

Different blends of Diesel and OME (Oxymethylene dimethyl ether) have been used for the single cylinder search engine. The latter are a class of DME (Dimethyl ether) derivatives that include different groups of oxymethylene (-O-CH2-) in the molecule [29]. OME compounds can be mixed with diesel fuel because of their higher molecular mass and boiling point. Two types of this fuels are used in this test: OME1 and OME3.5.

As it can be seen from the Table 3.7, both types of OME have a higher percentage of oxygen by volume than the reference Diesel, as well as a lower heating value and a higher density than Diesel. However, the cetane number compared to Diesel is higher for OME1 but lower for OME3.5. This allows to have mixtures with a wide enough range of cetane number to analyze the combustion behaviour.

	Lower Heating Value	**Density 25°C**	**O2 mass fraction**	**Cetane Number**
	MJ/kg	kg/m3	%	-
Diesel	42.72	832.4	0.7	52.30
15 % OME1	38.59	867.60	9.2	56.50
26.5 % OME1	35.46	893.80	15.5	58.16
40% OME1	32.37	921.4	21.7	60.42
65% OME1	26.27	981.10	34.0	67.13
100% OME1	19.5	1057	47.6	79.24
20 % OME3.5	38.80	839.86	9.2	53.10
35 % OME3.5	35.87	843.505	15.5	51.08
50 % OME3.5	32.96	847.15	21.7	48.07
80 % OME3.5	27.22	854.44	34.0	37.00
100 % OME3.5	23.45	859.3	42.1	24.16

Table 3.7: Fuel properties of single cylinder research engine

3.1.3 Results and discussion

This chapter shows the results of the experimental analysis of the fuel properties influence such as cetane number, heating value, oxygen content and density on combustion characteristics.

Cetane Number

The effect of cetane number on combustion behaviour is evident. As expected, the cetane number has a particular influence on the ignition delay and 10% of Mass Fuel Burned (X10). From the Figure 3.3 it can be observed that as the number of cetane increases the ignition delay is reduced, as well as the crank angle of X10 is advanced. Analyzing the other combustion characteristics, a direct influence of the cetane number is not evident. For example, analyzing 50% of Mass Fuel Burned (X50) it can be observed that in some operational points it has a tendency to be advanced, as in the case of 2500rpm and 7bar. At other operating points the trend is not clear, such as 1000rpm and 7bar where it shows a delay for Fuel1 and an advance for Fuel2 compared to the reference Diesel. The same can be observed for the maximum peak pressure (p_{max}), the maximum pressure gradient (dp_{max}) and the maximum heat release rate (HRR_{max}).

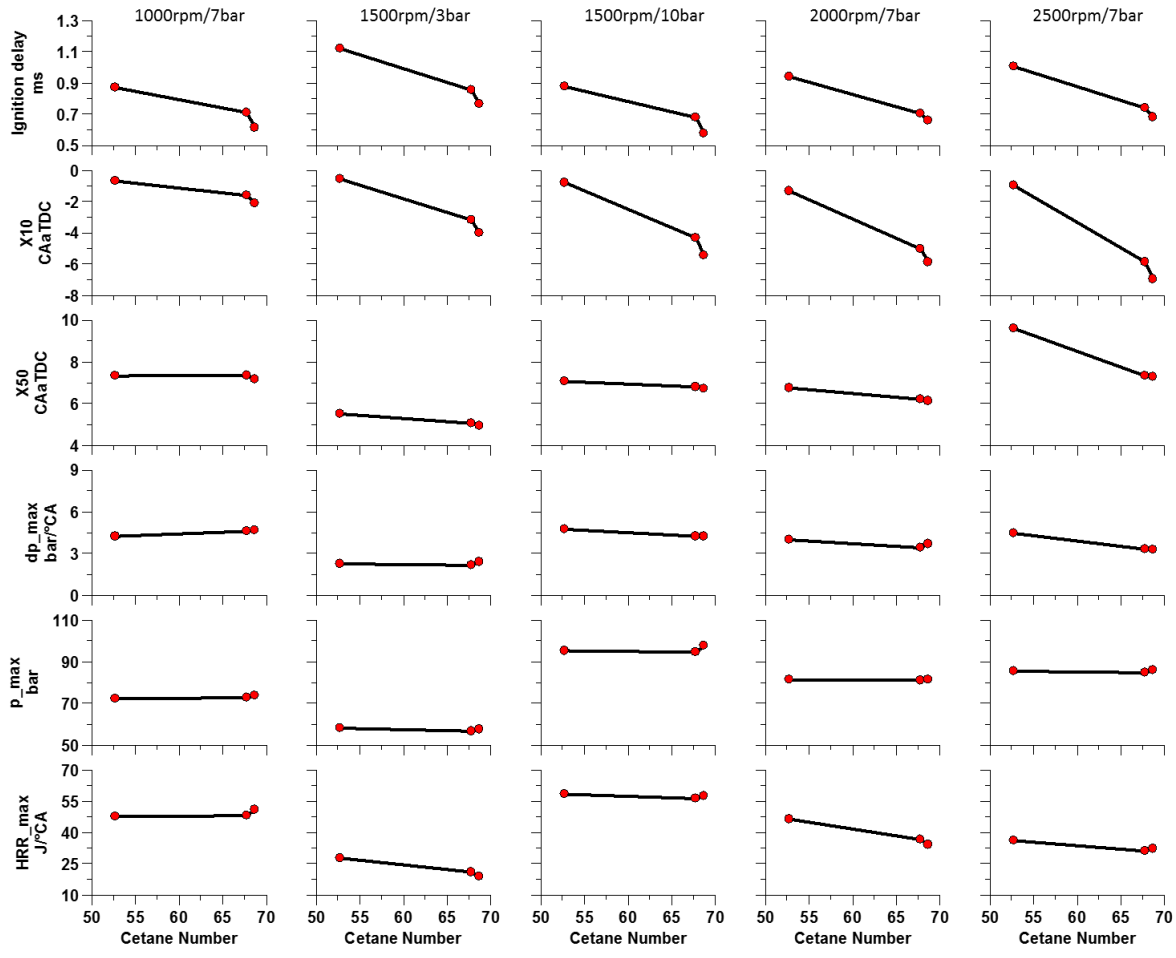

Figure 3.3: Effects of cetane number on combustion characteristics for 4-cylinder engine

The direct correlation of cetane number with ignition delay is due to the fact that a high cetane number means a higher ignitability of the fuel. Therefore, under equal thermodynamic conditions, this generates a reduction in ignition delay. The trend shown with the experimental analysis is the clear verification of this concept. Also, it can be noted that this trend is maintained for different engine speed and engine load.

The correlation with X10 is a direct consequence of the one with ignition delay. In fact, at the equal start of injection, a short ignition delay causes an advance of 10% of the burned mass. However, compared to ignition delay, X10 shows a steep trend at high engine speed while at low engine speed the trend is flatter. This may cause problems in identifying the cetane number at low engine speed if there are any changes in the X10 calculation, e.g. due to cycle to cycle fluctuations.

As for the 4-cylinder engine, a further analysis was carried out on the single-cylinder search engine with Diesel-OME flies to validate the results obtained. Also in this case, the direct influence of the cetane number on ignition delay and X10 is evident (Figure 3.4): the higher the cetane number, the shorter the ignition delay, and the more anticipated is X10. Instead no direct correlation of the cetane number with the other combustion characteristics is observed.

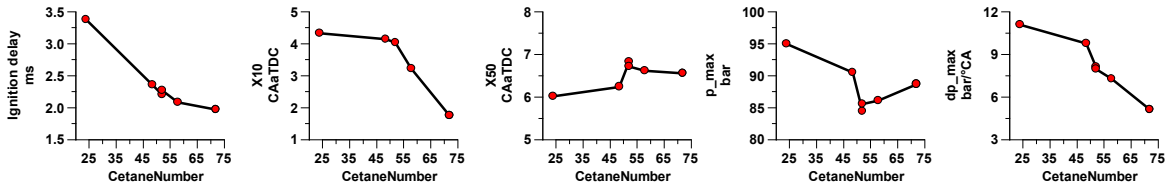

Figure 3.4: Effects of cetane number on combustion characteristics for single cylinder research engine

The findings confirmed with the two platforms allow to consider the two combustion characteristics, ignition delay and X10, as parameters to identify the cetane number and consequently the fuel.

Lower Heating Value

The test with the 4-cylinder engine shows a direct effect of the lower heating value with ignition delay and X10 (Figure 3.5). It is observed that for all engine operation points as lower heating value increases ignition delay is reduced and X10 is advanced. The same is not true for the other combustion characteristics X50, p_{max}, dp_{max}, HRR_{max}.

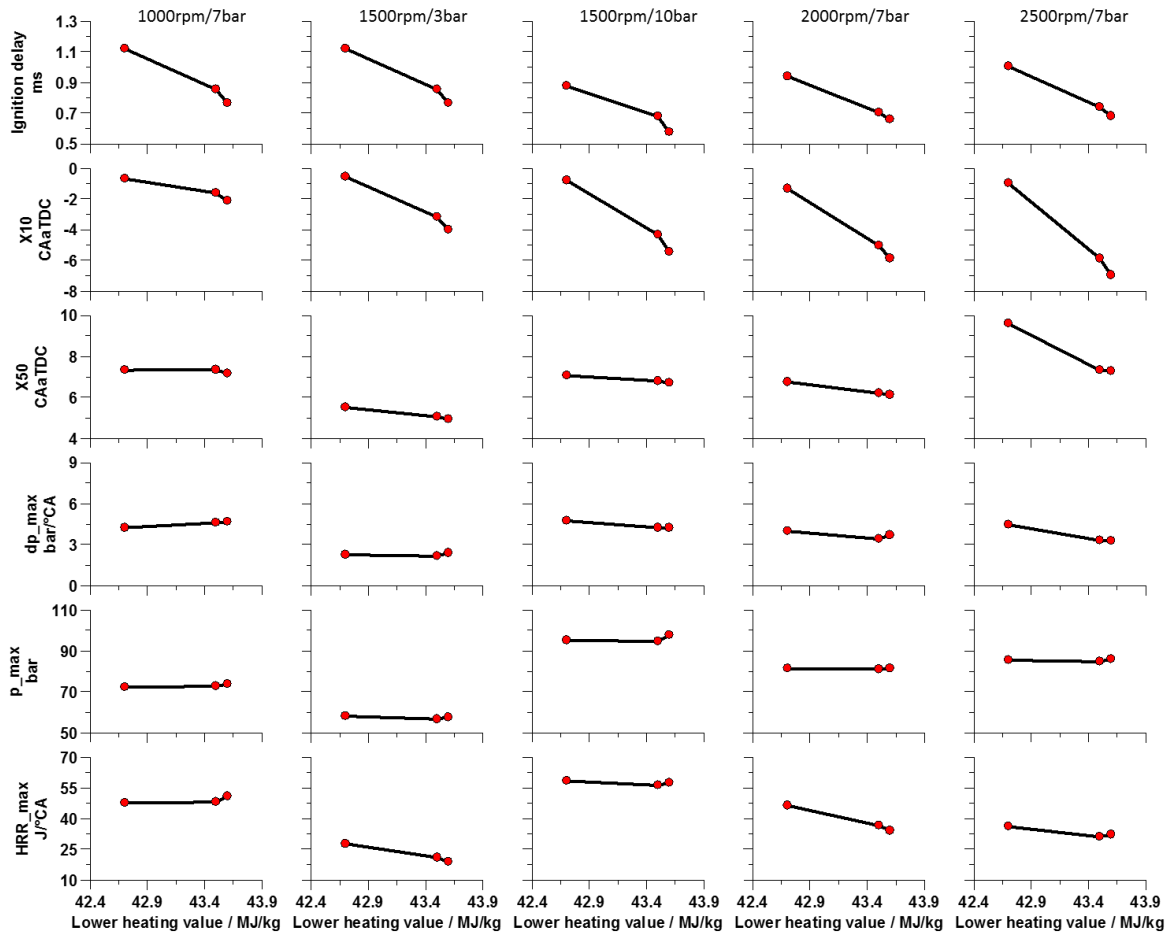

Figure 3.5: Effects of lower heating value on combustion characteristics for 4-cylinder engine

However, with the single-cylinder engine test this trend is not confirmed. In fact, from the Figure 3.6 we can see that there is no clear trend with the lower heating value.

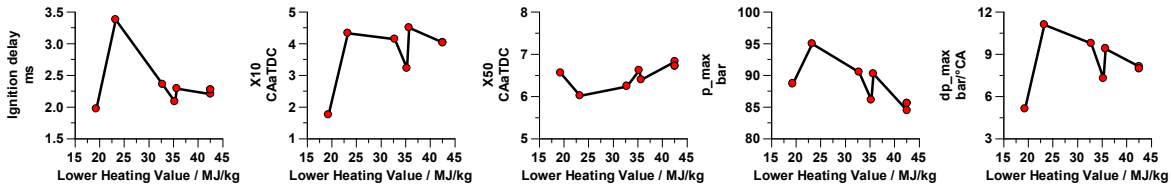

Figure 3.6: Effects of lower heating value on combustion characteristics for single cylinder research engine

This could be due to the fact that the change in the lower heating value influences other properties of the fuel and therefore it is not possible to isolate the influence of the lower heating value alone.

Density

The behaviour of the combustion characteristics with varying fuel density, for the 4-cylinder engine, is similar to that seen with the lower heating value and cetane number: In this case, as the fuel density increases, the ignition delay is longer and X10 is delayed (Figure 3.7). The other combustion characteristics, however, do not show a direct influence with the density.

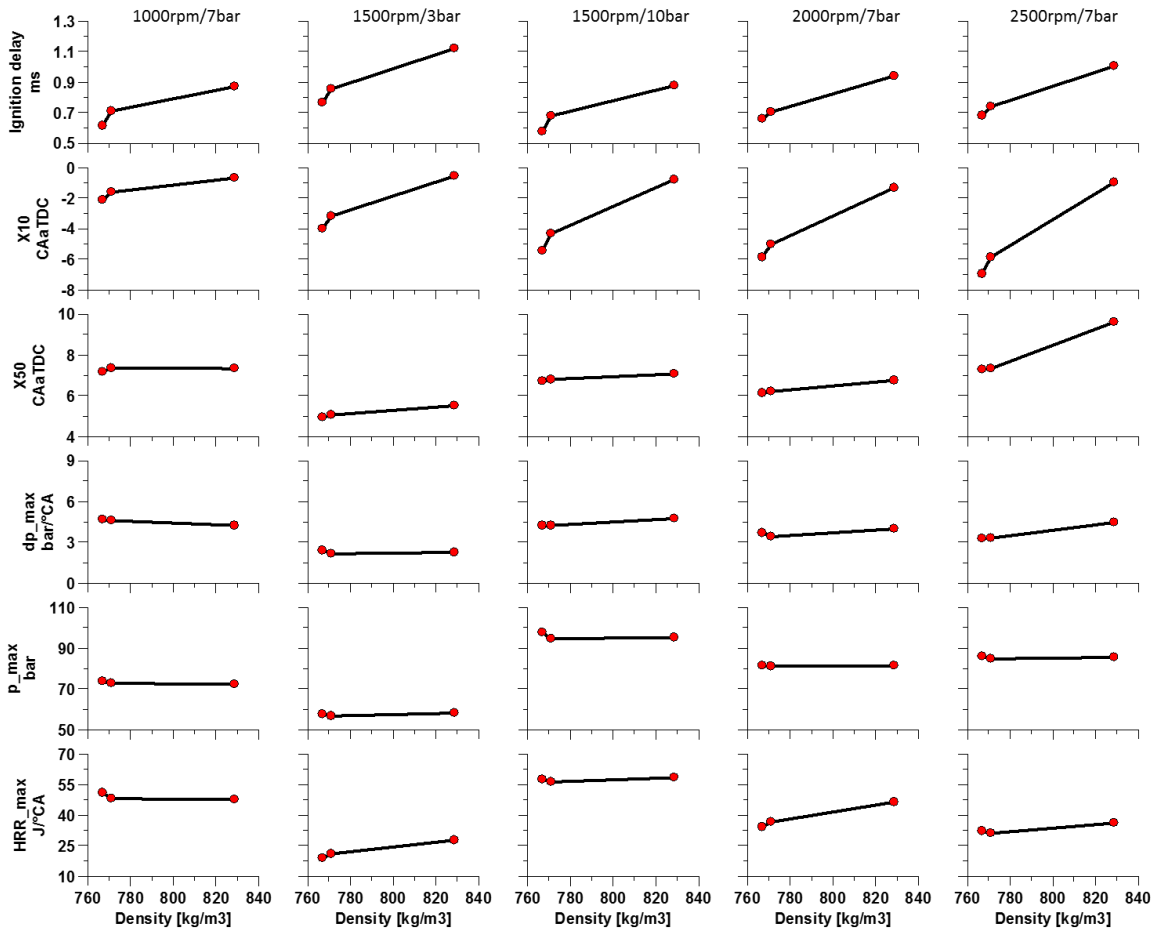

Figure 3.7: Effects of density on combustion characteristics for 4-cylinder engine

Similar to lower heating value, this trend is not confirmed with the second single-cylinder engine test. In fact, from Figure 3.8 no direct influence of density on combustion characteristics is observed.

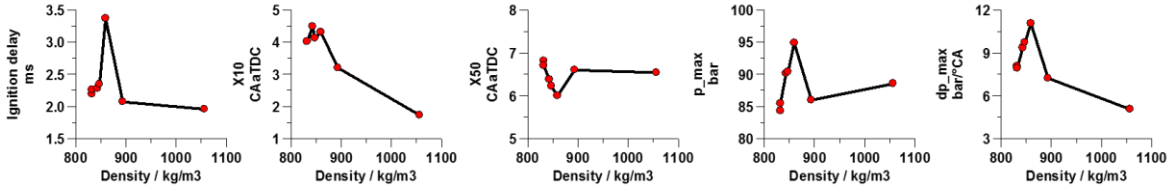

Figure 3.8: Effects of density on combustion characteristics for single cylinder research engine

Oxygen content

A further analysis was carried out on the influence of the fuel oxygen content on the combustion characteristics. What came out is that there is no direct correlation with the combustion behaviour, as can be seen in the Figure 3.9.

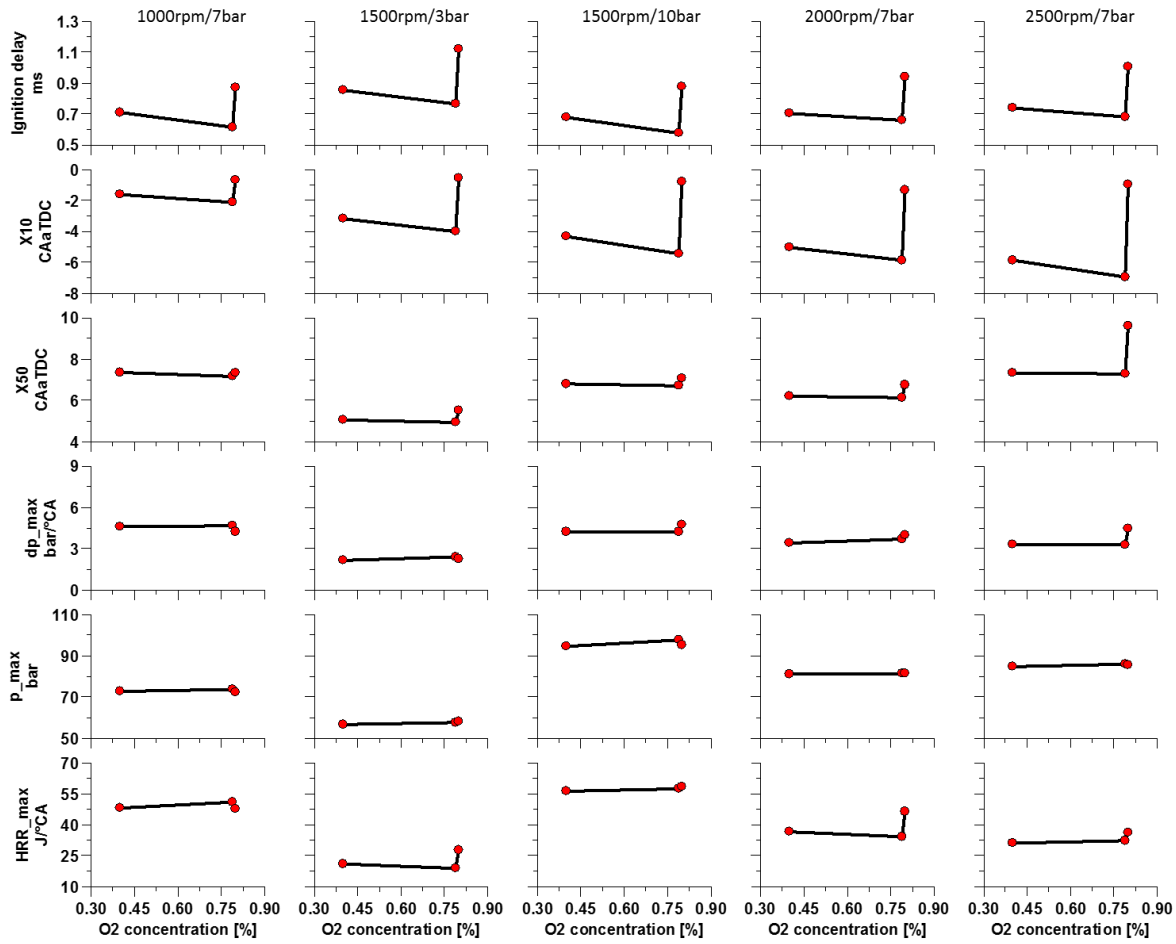

Figure 3.9: Effects of fuel oxygen content on combustion characteristics for 4-cylinder engine

Similarly, even on the test carried out on the single-cylinder engine, no direct co-relation of the oxygen content in the fuel with the combustion characteristics can be noted. This should be due to the fact that by varying the oxygen content other fuel properties also vary and therefore the variation of the oxygen content alone cannot be isolated.

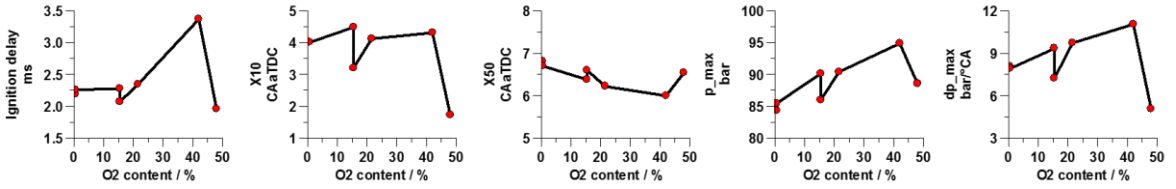

Figure 3.10: Effects of fuel oxygen content on combustion characteristics for single cylinder research engine

With the analyses carried out on both engines it is possible to reach the conclusion of the direct influence of the cetane number with the ability to ignite the fuel. This leads to a faster ignition of the fuel if the cetane number is higher and therefore in a shorter ignition delay and an earlier X10. Thus, ignition delay and X10 can be used as a criteria to detect cetane number and fuel.

3.2 Combustion characteristic sensitivity

The analyses performed in the experimental tests confirmed the direct correlation between cetane number and ignition delay and 10% of the burned mass. These combustion characteristics can be taken into account to identify the fuel running in the engine. In this chapter an analysis on which of the two is the most suitable for the purpose is made.

In order to figure out the robustness of the combustion characteristics, it is necessary to carry out a sensitivity analysis. With the tests carried out, in fact, it is possible to analyze them in relation to the cetane number.

The sensitivity analysis consists in evaluating the robustness of the combustion characteristics in case they change, for example due to cycle after cycle fluctuations, and how it could affect the identification of the fuel property, which in this case is the cetane number. Therefore, in order to carry out this analysis it is necessary to evaluate the variation of the cetane number as the combustion characteristics change. That is to highlight the gradient of the combustion characteristics by cetane number, described in the formula 3.6 and 3.7 as sensitivity factor (SF).

$$SF_{ID} = \frac{CetaneNumber_{max} - CetaneNumber_{min}}{IgnitionDelay_{max} - IgnitionDelay_{min}} \quad (3.7)$$

$$SF_{X10} = \frac{CetaneNumber_{max} - CetaneNumber_{min}}{X10_{max} - X10_{min}} \quad (3.8)$$

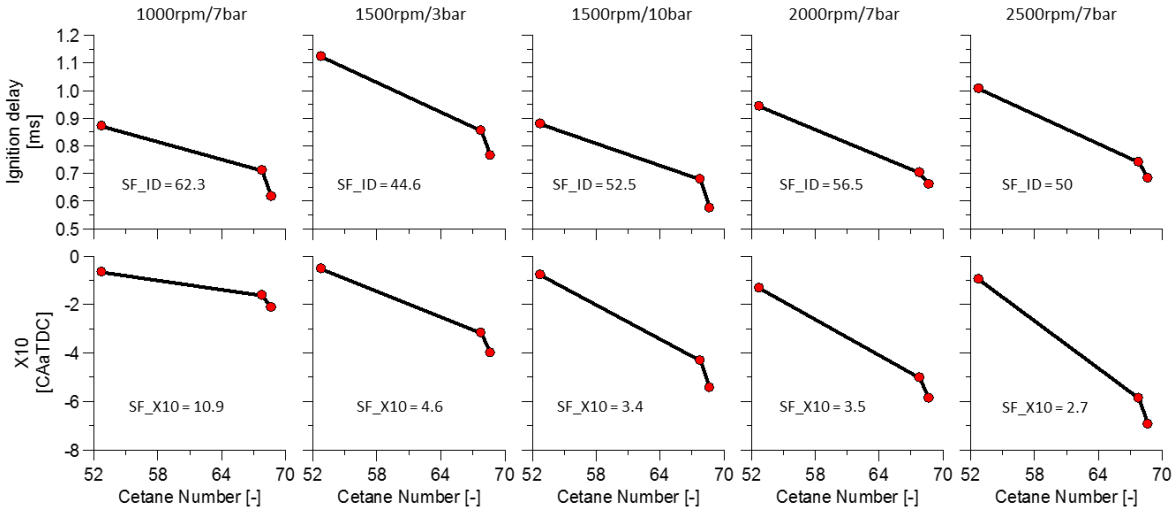

Figure 3.11: Sensitivity factor for ignition delay and X10

Figure 3.11 shows the values obtained for the two combustion characteristics for each engine operation point. It can be observed that the higher the Sensitivity Factor the more sensitive is the variation of the cetane number to the variation of the combustion characteristics. For example, for

the engine operation point of 1000rpm and 7bar, a one millisecond variation of the ignition delay can lead to a cetane number variation of 62.3, while a variation of one degree crank angle can lead to a cetane number variation of 10.9. In the Table 3.8 are reported max and min Sensitivity Factor for each combustion characteristic.

Sensitivity factor	unit	Max	Min
SF_{ID}	CN/ms	62.29	44.60
SF_{X10}	CN/deg	10.94	2.66

Table 3.8: Max and min Sensitivity Factor for ignition delay and X10

However, in order to understand which combustion characteristic shows greater robustness, it is necessary to identify possible variations of them and analyse what impact they have on cetane number. In order to do this, a possible variation of the combustion characteristics has first been assumed. With the maximum and minimum Sensitivity Factor values it is then possible to obtain the worst and best case of cetane number variation for each variation of the combustion characteristic assumed.

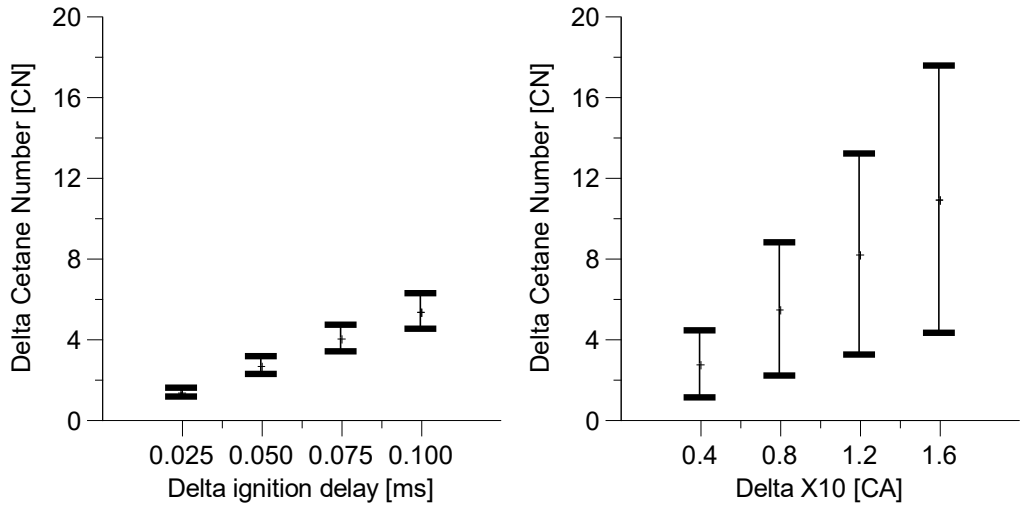

Figure 3.12: Cetane Number variation under combustion characteristics variation assumed

In the Figure 3.12 the variation in cetane number under the assumption of the variation in combustion characteristics can be observed. For example, with the 1.2 crank angle degree variation for X10 in the worst case scenario results a cetane number variation of 12. Ignition delay shows a higher robustness than X10. In fact, with a considerable variation of 0.1 ms of ignition delay, the cetane number deviation is contained below 4.

One way to verify that the assumptions made are realistic is to carry out a cycle-to-cycle analysis, deriving the deviations that can be found in the combustion characteristics.

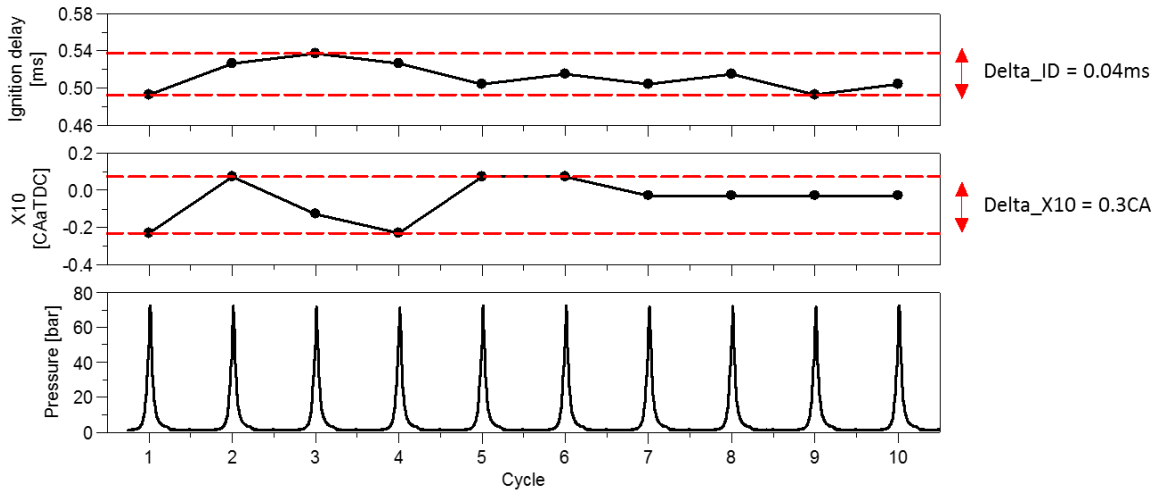

Figure 3.13: Cycle-to-cycle analysis for combustion characteristics deviation

Figure 3.13 shows an example of a cycle-to-cycle analysis of combustion characteristics over 10 cycles. It can be observed that the ignition delay deviation is 0.04 while that of X10 is 0.3 degrees crank angle. For each engine operation point each combustion characteristic has been derived cycle to cycle in order to have the deviation along the cycles. Afterwards, by multiplying the deviation with the corresponding Sensitivity Factor the deviations of the cetane number can be obtained.

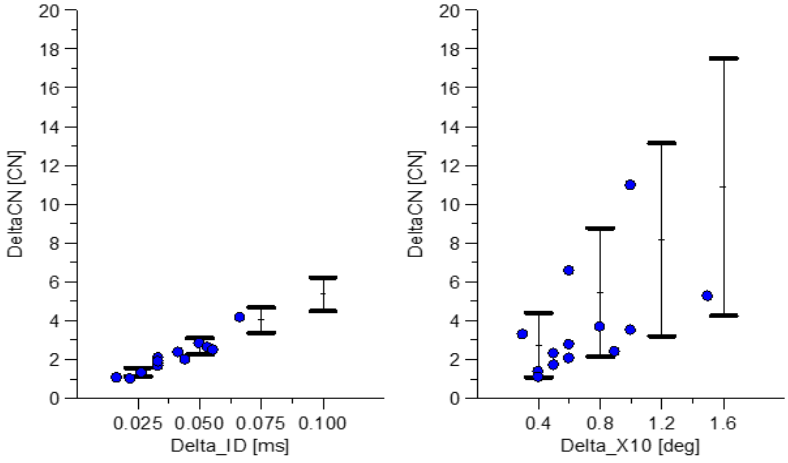

Figure 3.14: Cetane number deviation with cycle-to-cycle analysis

From Figure 3.14 it can be seen that the assumptions made were realistic and in addition ignition delay is confirmed to have a higher robustness. In fact, with this cycle to cycle analysis a maximum deviation of the ignition delay of 0.07 ms is shown, which leads to a deviation of the cetane number of 4, much less than one for X10, where we reach a deviation of the cetane number of 11. Moreover, another aspect can be highlighted: in fact the ignition delay error has a linear trend with the

deviation of the cetane number, while the error of X10 has a divergent trend, so even a small deviation can lead to a large variation of the cetane number.

3.3 Fuel identification function

As expected, a direct influence of cetane number with ignition delay and a crank handle of 10 % of the burned mass was found. This is mainly due to the definition of cetane number which indicates how easily a fuel ignites. In addition, regarding fuel variation, it has been observed that ignition delay shows a higher robustness than X10. In fact, in case of deviations of combustion characteristics, due for example to pressure signal noise, ignition delay has a lower impact than X10. Therefore, with these analyses, a model has been implemented that is able to predict the cetane number and therefore the corresponding fuel. Fuel identification allows the ECU to adapt different strategies (start of injection, fuel quantity, EGR rate, etc.) according to the fuel running in the engine, in order to have higher efficiency and lower pollutant emissions.

3.3.1 Function concept

The concept used to implement the model is based on calculating the current ignition delay and comparing it with the reference one. The cetane number is obtained as a function of the ignition delay deviation as shown in Figure 3.15.

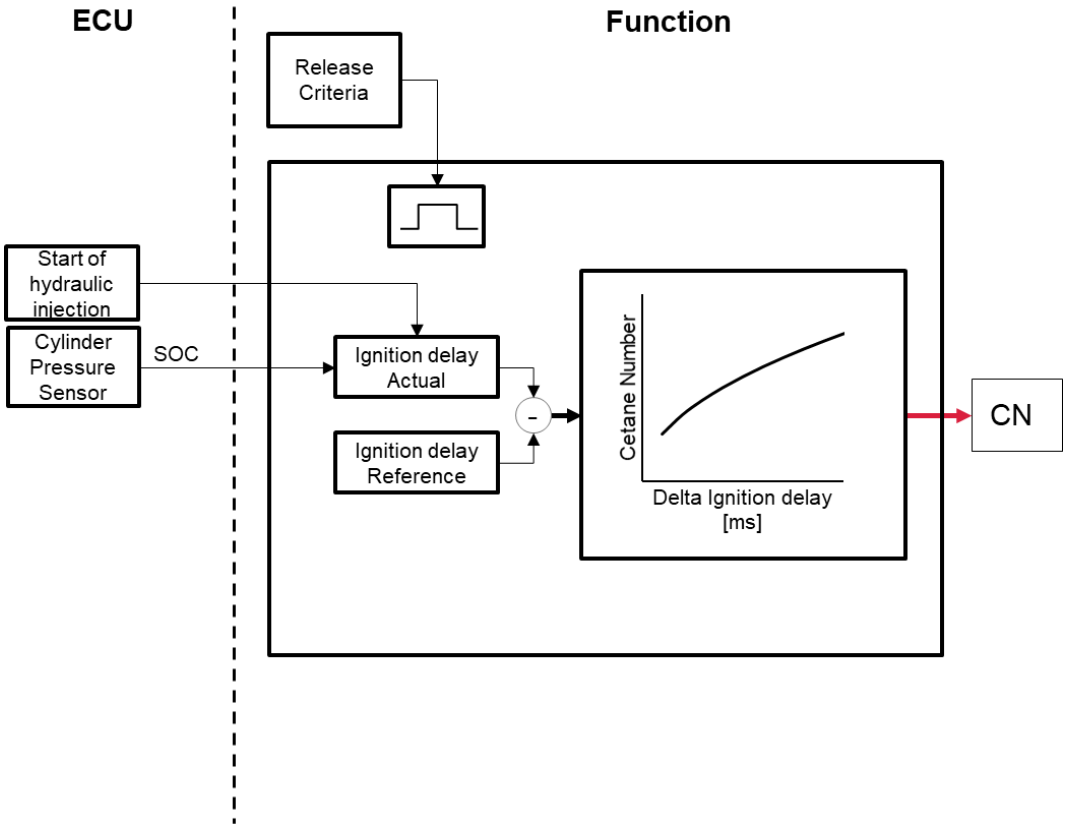

Figure 3.15: Function concept for cetane number detection

The current value of the ignition delay can be obtained from the difference of SOC and start of injection as previously discussed. The latter is obtained from the signal of the Start of Electric ECU to which the injector opening delay is added. The SOC, instead, is obtained from the in-cylinder pressure sensor, calculating the Heat Release Rate and detecting the first position the position where the heat release starts. This value compared to the reference value gives us the ignition delay deviation and consequently the cetane number associated with it.

However, ignition delay is strongly influenced by engine operation point and in particular by thermodynamic parameters such as temperature, gas pressure, rail pressure and oxygen concentration. Therefore, it is appropriate that the reference value to be compared with the current one is relative to the corresponding engine operation point or to the corresponding thermodynamic parameters.

Thus, the function must be activated under specific engine operation point or specific thermodynamic parameters. The Table 3.9 shows the possible release criteria of the function with the calculated reference value and what the characteristics of the function are in terms of complexity, robustness and flexibility. Complexity means the time and space used by the function and the computational effort required for the calculation. Robustness is the ability of the function to predict the calculated parameter with a low margin of error. Flexibility means the adaptation of the function to different input conditions.

Option	Release Criteria	Ignition delay Reference	Complexity	Robustness	Flexibility
1.1	Engine operation point and conditions (e.g. Speed, load, coolant temperature)	Single Value	+	0	-
1.2		Multiple Values (e.g. engine map)	+	0	0
2.1	Thermodynamic parameter (e.g. pressure, temperature, O2 conc.)	Single Value	+	+	-
2.2		Multiple Values (e.g. engine map)	+	+	0
2.3		Ignition delay Model	0	++	+

Table 3.9: Release criteria options for function activation

Among the possible options analyzed in the Table 3.9, in the first two the identification of the fuel can be performed at one or more specific engine operation points. In both cases the function has a low complexity, due to the simplicity of the structure, a medium level of robustness and a higher

flexibility for the second option, because it is possible to identify the fuel at several operating points. The last three show that it is possible to identify the fuel in one or more combinations of thermodynamic parameters. For example, the function can be activated in a specific thermodynamic condition with certain temperature values, pressure, oxygen concentration or under different thermodynamic conditions. Also in this case the reference value can be a single value or several values, for example a map. Unlike the first two options under specific engine operation points, options 2.1 and 2.2 have a higher robustness, since ignition delay is strongly influenced by thermodynamic conditions. In fact, the engine operation point determined to identify the fuel could be reached for example with a different EGR rate, thus varying the oxygen concentration and the previously calibrated reference ignition delay would be wrong for fuel identification. These situations can be encountered for example for cold start or DPF regeneration, where the ECU applies a different combustion strategy and consequently ignition delay is different from the reference ignition delay calibrated in steady state.

The last option shown in the Table considers the activation of the function under specific thermodynamic conditions, but the ignition delay reference value is calculated using a model instead of being calibrated in lookup table. In this way it is possible to have a greater robustness and flexibility even if a more complex function. It has a greater robustness because in order to activate the function in the previous cases, tolerances in the release criteria parameters are necessary. For example, a specific engine operation point may not be reached exactly by never activating the function, so it is necessary to have a tolerance window so that the release criteria can be reached. This tolerance, however, may lead to a different ignition delay due to different inputs, leading to a fuel prediction error. With ignition delay model the reference value is calculated online, thus obtaining a higher accuracy. Moreover, with this last option flexibility is higher because with the real time calculation of the reference value it is possible to predict the fuel in any condition and not be bound only to some calibrated conditions.

3.3.2 Ignition delay calculation approach

The ignition delay calculated so far follows the standard definition of difference between start of combustion and start of injection. However, if identifying the start of injection is feasible via the start of electric and opening delay, identifying the start of combustion is not a real time parameter. In fact in most cases, due to the pressure signal noise, the identification of the exact combustion start point is subject to errors. To avoid this, 10% of the burnt mass can be considered as the start of combustion, since X10 is easily identifiable with the cumulative Heat Release Rate, which is less influenced by the noise of the pressure signal. The new definition can be seen in Figure 3.16 on the left: the three ignition delays for the three fuels are highlighted.

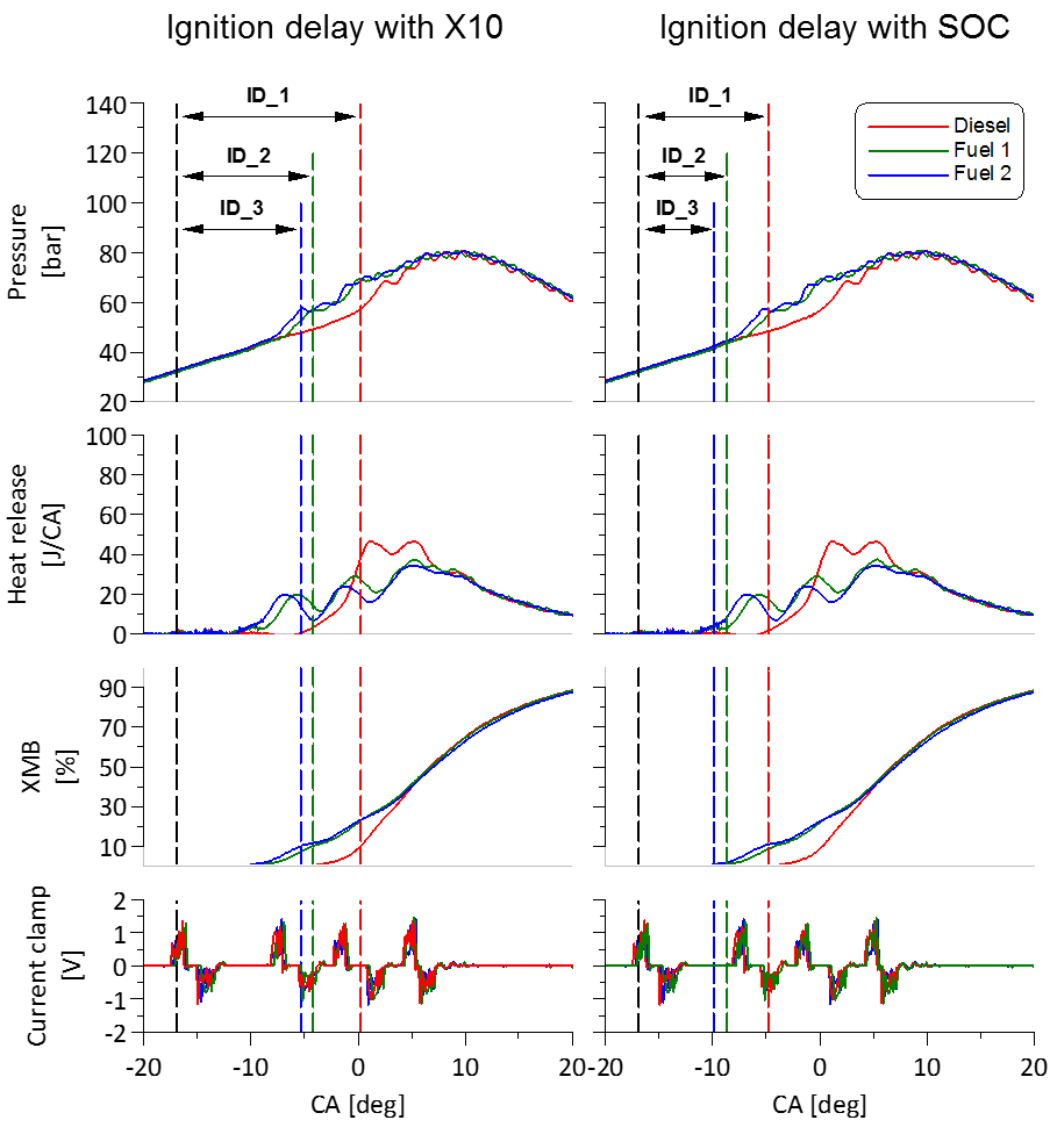

Figure 3.16: Ignition delay definition with X10

This new definition of ignition delay also maintains the same behaviour when the fuel changes. In fact, as can be seen in Figure 3.17, the new ignition delay maintains the same trend as the standard definition: it decreases with increasing cetane number.

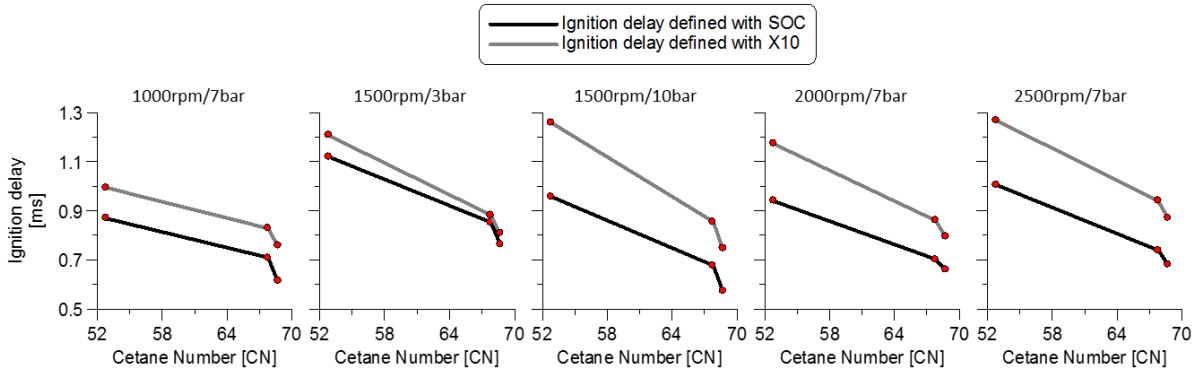

Figure 3.17: Influence of cetane number on the new ignition delay

The use of parameter X10 directly is rejected because, as previously analysed, it has a lower robustness than the ignition delay in case of disturbances to the pressure sensor. This is mainly due to its dependence on engine speed: in fact, as seen in Figure 3.11, at low engine speed X10 has a low variation when the fuel changes, while at high engine speed the variation is more evident. This influence from engine speed is not found on ignition delay, which has a constant trend at different engine speeds.

3.3.3 Ignition delay model

Each fragment of fuel injected goes through several intermediate mechanisms until it is ready for self-ignition [30]. The time duration of this chain of mechanisms refers to the ignition delay, i.e. the duration between the start of hydraulic injection and the start of combustion. The ignition delay is divided into a physical and a chemical part, Figure 3.18.

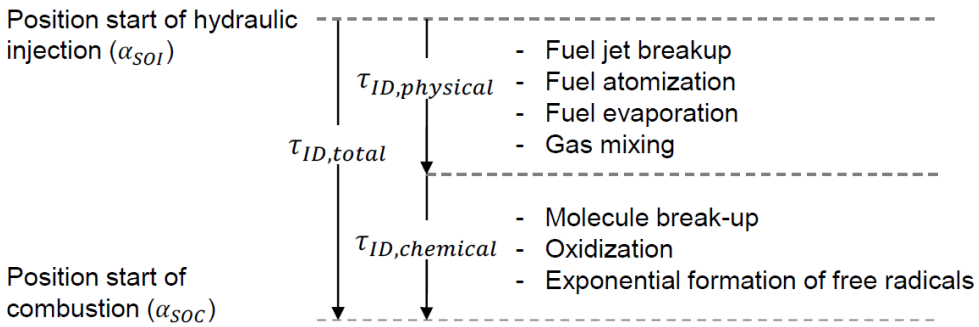

Figure 3.18: Ignition delay mechanisms according to [30]

When the fuel comes out of the injector nozzle, it has a high speed in relation to that of the cylinder gas. This high relative speed causes an initial fuel jet break-up near the injector nozzle due to cavitation effects within the injector nozzle, aerodynamic forces and fuel jet instability [31] [32] [33]. This initial stage of fuel jet break-up is referred to as primary break-up. The second break-up phase consists of atomization, i.e. the formation of small fuel droplets. The formation of fuel droplets is essentially governed by the physical properties of the fuel, such as viscosity, surface tension [34]. Once the droplets have heated up, the fuel evaporates and mixes with the surrounding gas, initiating chemical reactions between oxygen and fuel molecules. These oxidation processes exothermically break the larger hydrocarbons into smaller molecules, resulting in exponential formation of free radicals, which generates the thermal explosion [11]. Therefore, the length of the total ignition delay is considered as the sum of the chemical and physical ignition delay, equation 3.8.

$$\tau_{ID} = \tau_{chemical} + \tau_{physical} \qquad (3.9)$$

Both ignition delay parts are modeled separately. The validity of the ignition delay model is finally demonstrated by experimental engine test data. Ignition delay measurement, calibration and validation are carried out using the workflow shown in Figure 3.19. The ignition delay is defined as the time difference between the hydraulic start of injection and the start of the heat release event. The start of the hydraulic fuel injection position (αSOI) is derived from the start of the electric injection actuation considering the opening delays related to the injector. Ignition delay models are generally used to predict the ignition delay behaviour based on the gas states in the thermodynamic cylinder at the α_{SOI} position or through an integral consideration of the gas states between the αSOI positions and the start of combustion (α_{SOC}).

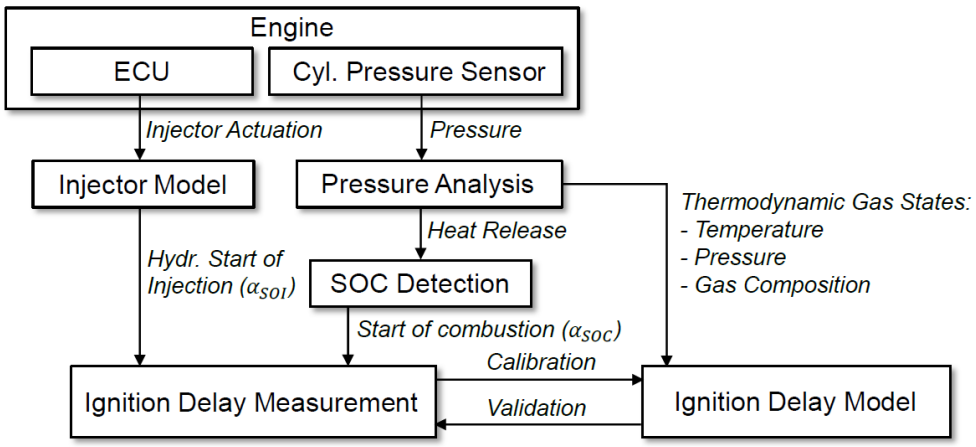

Figure 3.19: Workflow of ignition delay model calibration and validation

Regarding ignition delay measurement, the position α_{SOC} is defined as the individual start of combustion event. Once the position α_{SOC} has been determined, the ignition delay can be obtained according to its position α_{SOI}. The ignition delay detection method is shown graphically in Figure 3.20 for an exemplary engine operation point.

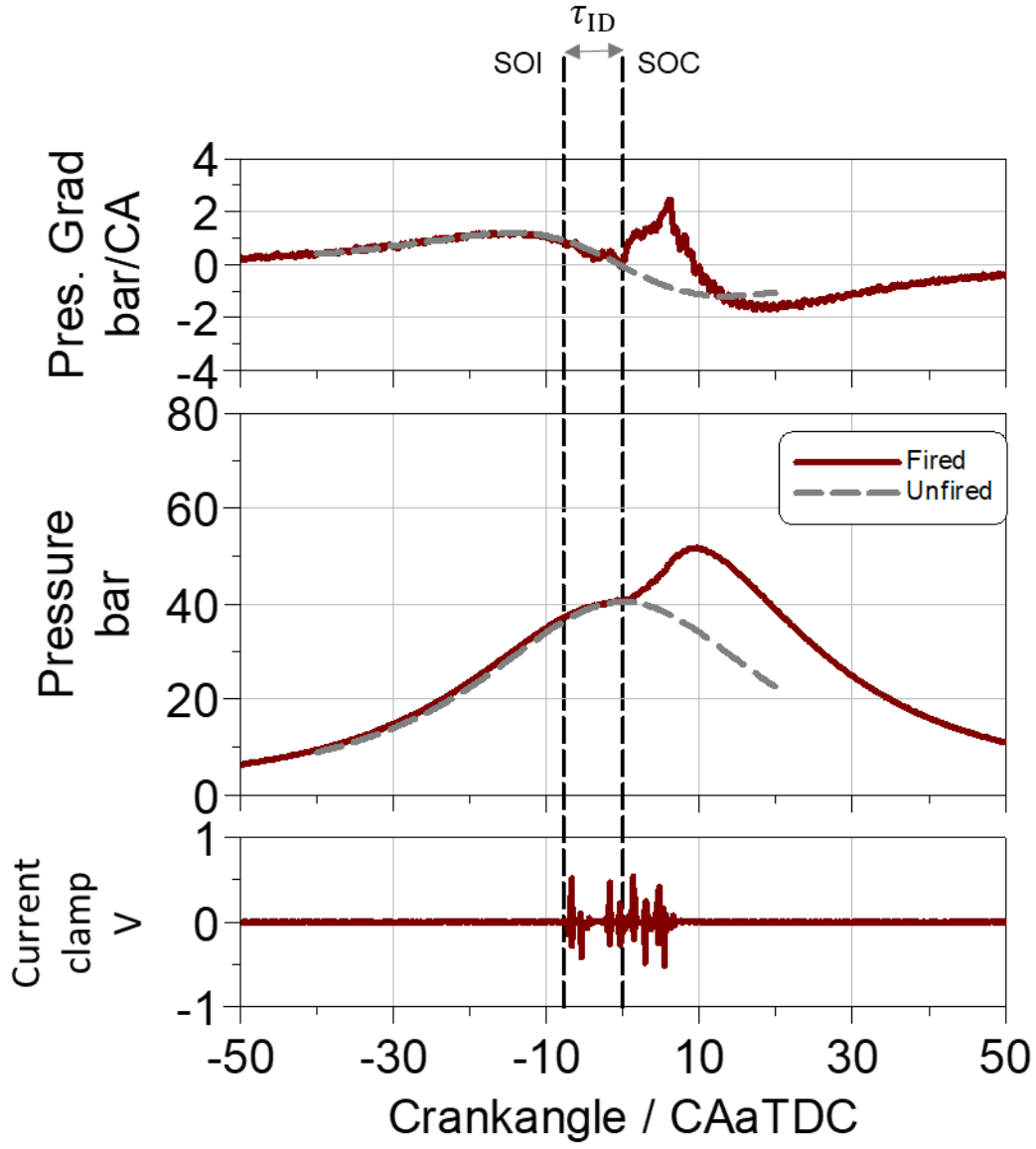

Figure 3.20: Ignition delay detection method (n = 1000 rpm, $IMEP_g$ = 7 bar, EGR, p_2 = 2 bar, p_{rail} = 1000 bar)

As discussed above, the ignition delay can be modelled in two parts, the chemical and the physical. The part of the chemical ignition delay considers the molecular chain break-up and the chemical mechanism, which includes the formation of free radicals [35]. The kinetics of the chemical reaction follows a low or high temperature path. The high temperature path is considered as a single-stage reaction with an instantaneous chain break independent of the fuel structure. The low temperature auto-ignition path follows a multi-stage reaction pattern that can be reduced in three stages according to Figure 3.21.

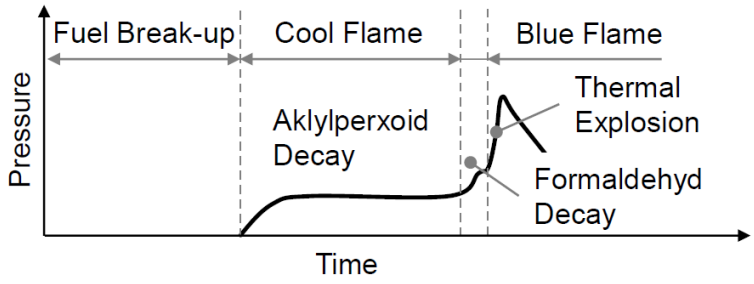

Figure 3.21. Self-ignition process of the low-temperature path within a homogenous reactor according to [7]

During the fuel molecule break-up phase, large fuel molecules begin to break down into Alkylperoxid, which is a relatively stable intermediate product. Once a critical concentration is reached, the decay of Alkylperoxid begins. The critical concentration of Alkylperoxid decreases with increasing temperature, so the duration of this phase also decreases.

The transformation of Alkylperoxid into Formaldehyde is an exothermal process that develops reactive free radicals, thus showing an explosive character. This phase refers to the cool flame process and can account for up to 15% of the total fuel conversion of the system [7]. The intensity of the cool flame increases with a higher initial concentration of Alkylperoxid, i.e. a lower temperature, which results in a shorter duration of this phase. As a result, the cool flame phase shows a contrary behaviour to the fuel break-up phase. The occurrence of the cold flame phase is observed in a variation of the injection timing of the experimental data of the steady state engine test, Figure 3.22.

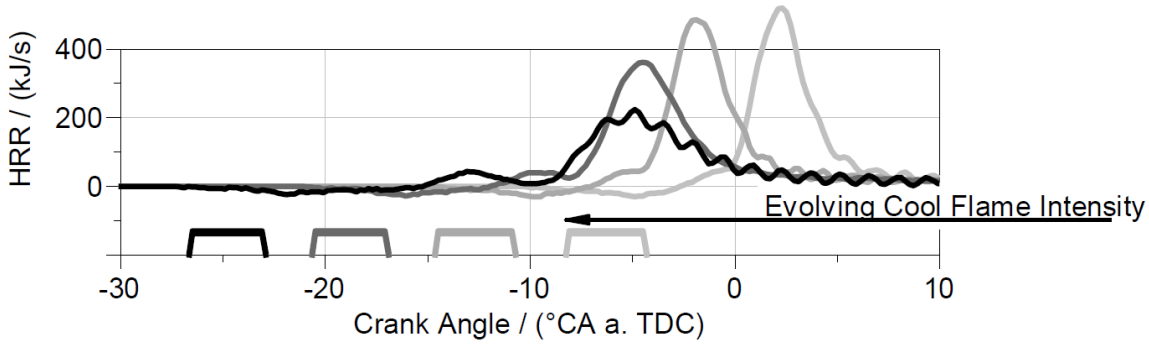

Figure 3.22: Cool flame phase occurrence via variation of main injection timing (n=1500 min–1, $IMEP_g$=9.4 bar, no EGR, p_2=2.3 bar, p_{rail}=800 bar)

An advanced main injection timing causes cooler gas temperature conditions during the ignition delay. According to the theory of the cool flame phase phenomenon, the peak of the initial heat release rate intensifies due to a higher critical Alkylperoxid concentration.

Formaldehyde is converted exothermically into carbon monoxide during the blue flame phase. The expression blue flame corresponds to the fact that the characteristic radiation spectrum of Formaldehyde shines blue during its oxidation process. A high number of free radicals are produced during this process, allowing instantaneous CO oxidation with the residual oxygen, causing a thermal explosion. This thermal explosion indicates the start of combustion. The duration of the blue flame phase is small compared to the fuel break-up phase and the cool flame phase, so the duration of the blue flame phase is generally neglected compared to the other two.

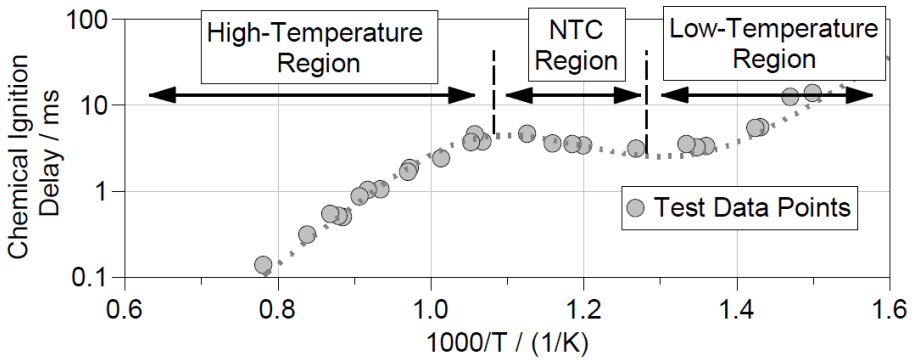

Figure 3.23: Measured chemical ignition delay from a shockwave tube for n-Heptane at 13.5 bar and an air/fuel equivalence ratio 1.0 according to [36] [37]

The temperature dependency on the chemical ignition delay in the low-temperature region is mainly influenced by the fuel molecule break-up phase and the cool flame phase. These two phases show a controversial behaviour in terms of temperature dependency. As the temperature increases, the duration of the fuel molecule break-up phase decreases, while the duration of the cool flame phase increases. Considering Figure 3.23 and starting from a low temperature point, the chemical ignition delay decreases to the local minimum as the temperature increases. This is due to the dominance of temperature dependence on the break-up phase of the fuel molecule in that region. From the local minimum point, increasing the temperature there is an increasing ignition delay due to the predominant temperature influence of the cool flame phase. This temperature range is known as the negative temperature coefficient (NTC) region. Once the maximum local temperature is reached, the transition from the low temperature ignition delay path to the high temperature path occurs. Any increase in temperature from that point causes a decreased chemical ignition delay.

In addition to the influence of temperature on chemical ignition delay, other parameters such as pressure and oxygen concentration are taken into account, as shown in the equation 3.9.

$$\tau_{chemical} = k_1 \cdot \left(\frac{p}{p_{ref}}\right)^{l} \cdot \left(\frac{O_2}{O_{2,ref}}\right)^{m} \cdot \left(\frac{T}{T_{ref}}\right)^{n} \cdot e^{\frac{T_{Ea}}{T}} \quad (3.10)$$

Both are correlated to a basic value in order to improve calibratability. By choosing an ignition delay data set at base pressure (p_{ref}) and oxygen concentration level ($O_{2,\,\mathrm{ref}}$), the activation energy (Ea) and reaction rate (k_1) are calibrated without the influence of pressure or oxygen concentration. An individual change in pressure and oxygen concentration can then be carried out to calibrate the remaining exponents (*l,m*) for the influence of pressure and oxygen concentration.

The equation is based on a typical Arrhenius [7] approach to capture the exponential influence of temperature, pressure and oxygen concentration on the behavior of chemical ignition delay.

Regarding the physical ignition delay time, it is mainly determined by the duration of the fuel jet break-up and fuel droplet evaporation phases [35]. The mixing between the resulting fuel vapour and the gaseous phase is considered an instantaneous task, which takes place in parallel with the break-up phase of the fuel jet and the evaporation phase itself [35].

The fuel jet break-up time describes the duration between $\mathrm{SO}I$ and the break-up of the fuel jet in droplets with a characteristic diameter. The break-up time of the fuel spray is calculated considering the fuel spray penetration length, i.e. the distance between the tip of the injector nozzle and the top of the fuel spray cloud. According to [38], the break-up behaviour of the fuel spray is influenced by the rail pressure, the layout of the injector nozzles and the gas density. The resulting collective of fuel droplets after fuel jet breakup typically inherits a change in droplet size, which are larger within the core of the fuel jets and smaller around the contour phases between fuel and gas due to the higher gas shear forces.

Therefore, the physical ignition delay time is modelled from equation 3.16, considering the same approach used for the chemical ignition delay. Therefore, the physical ignition delay time is modelled from equation 3.10, considering the same approach used for the chemical ignition delay. Cylinder and rail pressure are correlated to a reference value and exponents in order to improve calibratability.

$$\tau_{physical} = k_2 \cdot \left(\frac{p}{RT\rho_{ref}}\right)^{r} \cdot \left(\frac{p_{rail} - p}{p_{rail,ref}}\right)^{s} \quad (3.11)$$

Since no individual measurements of chemical or physical ignition delays are available, an iterative calibration approach is conducted for a simultaneous calibration of both ignition delay parts, Figure 3.24.

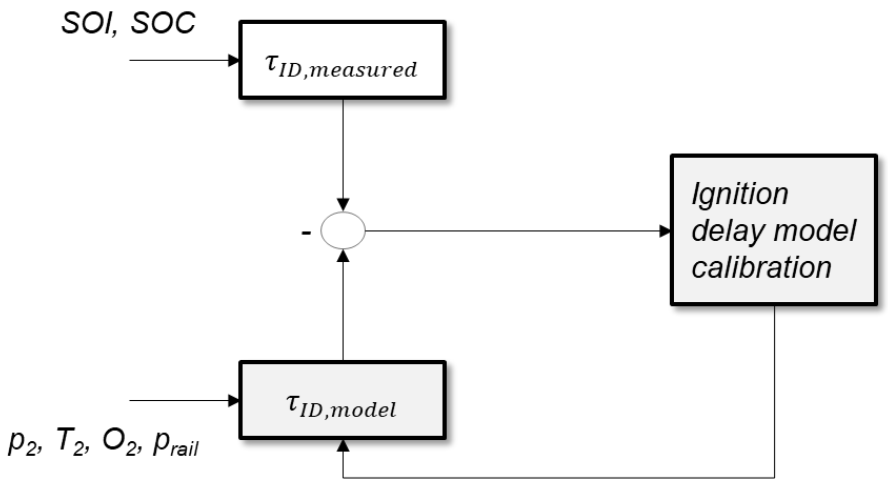

Figure 3.24: Ignition delay model calibration procedure

The calibration procedure consists of comparing the ignition delay value measured with the ignition delay value calculated by the model. For each engine operation point the positions of SOI and SOC are collected in order to have the measured ignition delay value. In addition, for the same engine operation points, data of pressure and temperature intake manifold, oxygen concentration and rail pressure are collected. Calculating ignition delay with the equations 3.9 and 3.10, the exponential parameters (l,m,n,r,s) and incidence parameters (k_1,k_2) of the two rates are calibrated in order to have a prediction as close as possible to the measured one.

The resulting model performances of the complete ignition delay model are shown in figure 3.25. The correlation is evaluated in terms of the coefficient of determination (R^2).

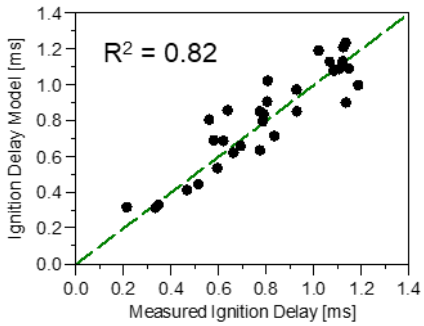

Figure 3.25: Ignition delay model performance

The ignition delay prediction obtained with the model shows high accuracy, and is therefore a good approach to use for the calculation of the reference ignition delay.

3.4 Function robustness

The combustion characteristics previously analyzed, useful to understand the combustion behaviour, can be obtained by a feedback signal of a cylinder pressure sensor. This type of

calculation does not require extra requirements of the cylinder pressure sensor, cylinder pressure sensors available in series in terms of stand-alone [39] or even in terms of an integrated glow plug solution [40].

In the present study, a piezoelectric pressure sensor was used to obtain the pressure signal and calculate the related combustion characteristics. Piezoelectric sensors use the piezoelectric effect, through which piezoelectric materials produce electrical potential when a mechanical load is applied. This type of sensor is considered a mature technology with exceptional reliability. The piezoelectric material has a high elastic modulus and therefore almost zero deflection and an extremely high natural frequency. In addition, it has excellent linearity over a wide amplitude range. However, all pressure transducers, regardless of their material composition, cost or accuracy, are susceptible to sensor drift over time. Pressure sensor drift is a gradual degradation of the sensor and other components that can make readings offset from the original calibrated state

Another phenomenon that could affect the calculation of the combustion characteristics is the presence of the pressure signal noise. This is due to many sources that can disturb the signal. F.Payri et al. [41] noted that with increasing engine speed, there is an increase in the energy level in the low, medium and high frequency components of the cylinder pressure signal.

To take into account the possibility of sensor drift, the pressure traces that the sensor can detect in the case of 12 sensor condition scenarios have been derived. The new combustion characteristics were then calculated and their robustness analysed. In parallel, the noise of the pressure signal was simulated in order to analyze how it affects the combustion characteristics and the cetane number detection.

3.4.1 Cylinder pressure sensor drift

The method used to simulate the drift of the pressure trace is based on experimentally obtained data from possible scenarios that the pressure sensor may face. In the Figure 3.26 the different scenarios tested for the sensor used are shown. The sensor was analyzed in three different temperature conditions: in a cold condition at -40°C that represents the cold start condition in very cold countries, in an ambient condition at 23°C and in a hot condition at 140°C that represents an engine overheating condition. In addition, for each temperature condition the positive drift, negative drift and unclean sensor conditions have been tested and compared with the normal operating condition with the clean sensor.

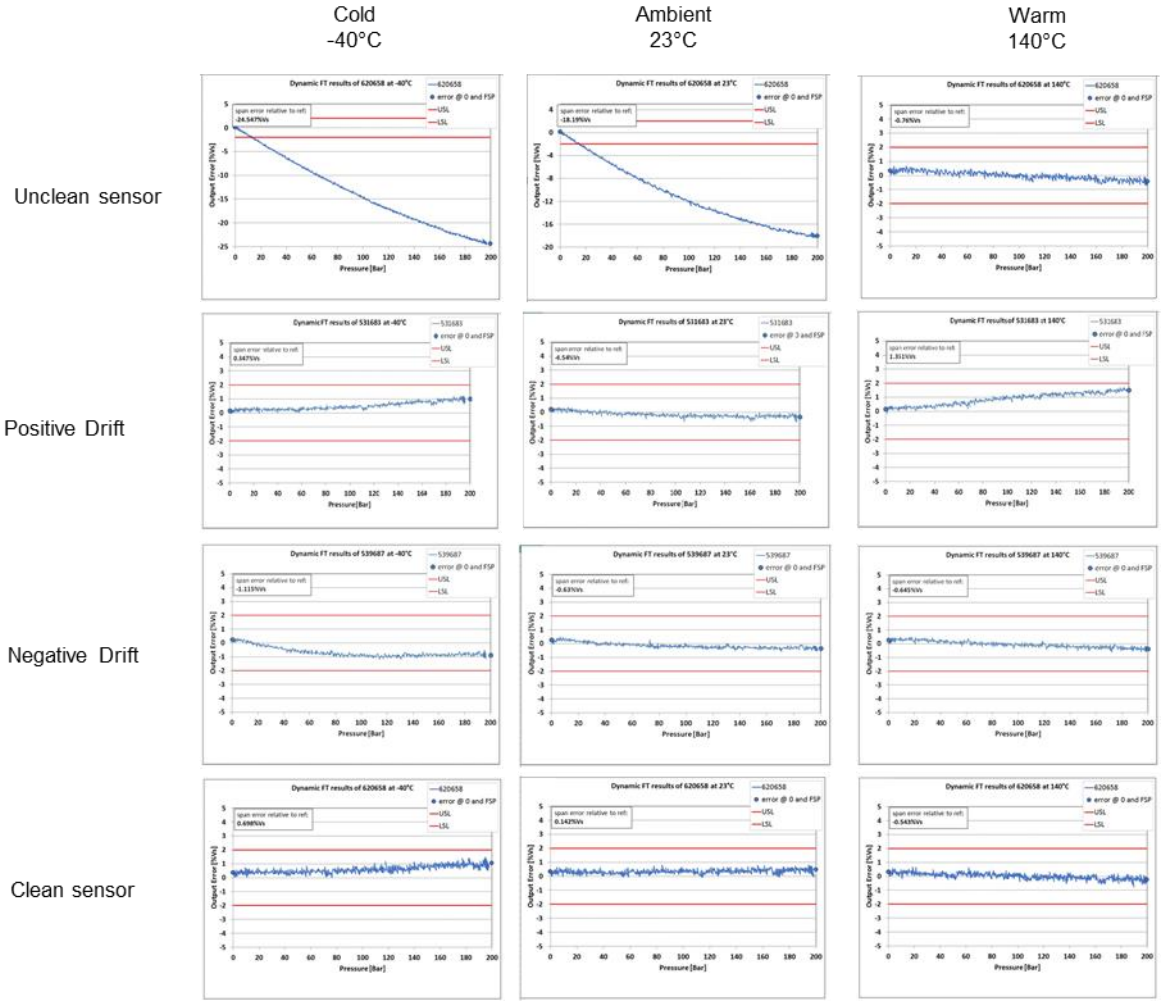

Figure 3.26: Experimental pressure sensor drift scenarios

In the figure the error generated in output by the sensor is a function of pressure. Therefore, to obtain the drift pressure traces it is necessary to derive the pressure delta as a function of pressure. To do this we use the transfer curve of the sensor defined with the formula 3.12

$$U = a * p + b \qquad (3.12)$$

where *a* is the gradient of the transfer curve and *b* is its offset.

With the definition of the transfer curve formula and its constants *a* and *b*, it is possible to obtain the pressure delta from the sensor output error using the formula 3.13

$$\Delta p\,(p) = \frac{\Delta U(p)}{a}(a * p + b) \qquad (3.13)$$

An example of the pressure delta generated under warm and positive drift sensor conditions is shown in Figure 3.27.

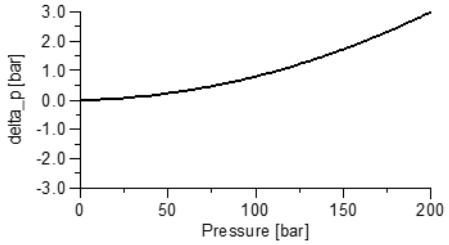

Figure 3.27: Delta pressure for warm and positive sensor drift condition

With the pressure delta caused by the sensor drift in the different scenarios described, the new drift pressure trace is obtained. The sensor drift simulation is described schematically in Figure 3.28.

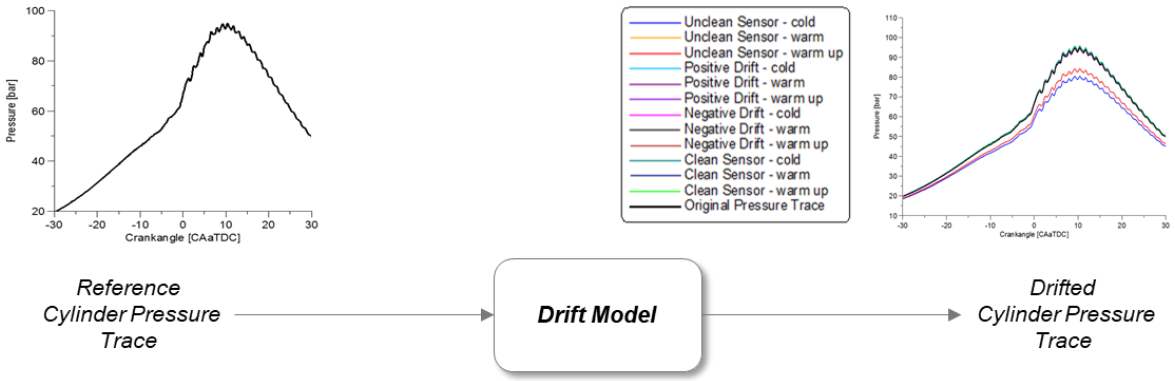

Figure 3.28: Schematic drift simulation

It can be seen that in the extreme case of an uncleaned sensor in cold temperature conditions, the pressure trace undergoes a considerable deviation, reaching 15 bar difference in the maximum pressure peak.

With the drift pressure traces it is possible to derive the pressure characteristics for each sensor condition. In our study, what interests us, according to the experimental analysis carried out previously, are the ignition delay parameters and 10% of the burnt mass (X10). For the calculation of this last parameter it is necessary to obtain the Heat Release Rate with the formula 3.3, neglecting the heat exchange with the walls. For the calculation of volume *V* we use the formula 3.14

$$V = r\left[(1-\cos\theta) + \frac{1}{\Lambda}\left(1-\sqrt{1-(\Lambda\sin\theta)^2}\right)\right]\frac{\pi}{4}d^2 + \frac{\frac{\pi}{4}d^2 c}{\varepsilon - 1} \qquad (3.14)$$

Where

- r: crank radius
- θ: crank angle
- Λ: rod ratio, ratio between crack radius and connecting rod
- d: cylinder bore
- c: engine stroke
- ε: compression ratio

By normalizing the cumulative Heat Release Rate, it is possible to obtain the value of 10% of the burned mass (X10), as shown in Figure 3.29.

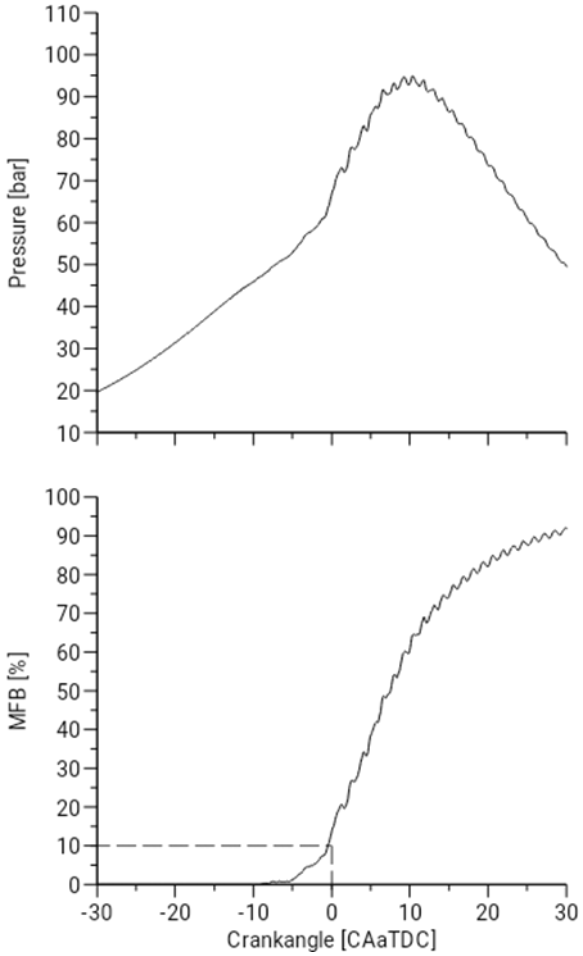

Figure 3.29: X10 calculation from pressure trace

3.4.2 Pressure signal noise

The pressure signal noise is the second phenomenon analyzed to validate the function. To simulate the pressure trace with the presence of noise, a noise signal based on a sinusoidal curve was generated, as described in the equation 3.15.

$$noise = A * sin\,(2\pi f) \qquad (3.15)$$

Where

- A: noise amplitude
- f: frequency

According to Pfluger [42], analyzing two types of sensor one of which is used for series applications, the minimum frequency from which you can see the signal noise is 850Hz. Moreover, Pfluger claims that the signal noise is load-dependent and this can be observed between 2000 and 3000 Hz over the frequency spectrum. So, by simulating the noise signal at these frequencies and with load dependence, this can be added to the reference pressure trace, as described in formula 3.16.

$$p_{noise} = p_{orig} + noise \qquad (3.16)$$

The simulation of the noise signal thus generates a significant disturbance to the original pressure trace, as can be seen in Figure 3.30 on the right, where the resolution has been increased to highlight the generated noise.

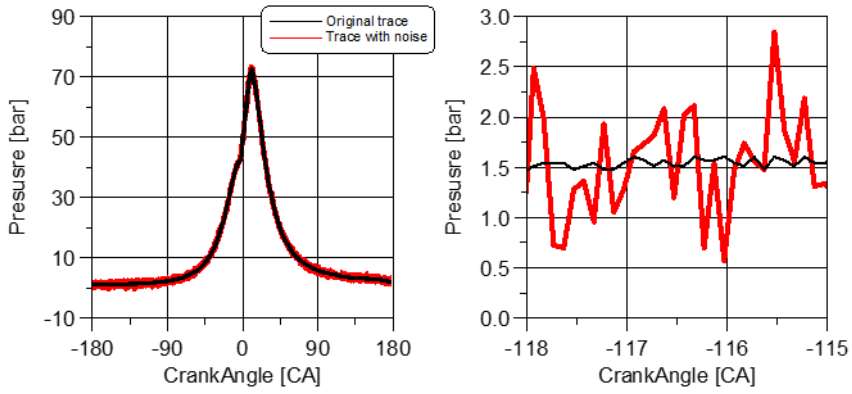

Figure 3.30: Pressure trace with signal noise simulated

The method of simulating pressure signal noise is described in Figure 3.31 schematically. In addition, the different noise signal is visible for high and low load: in the frequency spectrum a higher signal noise is noticed for high load.

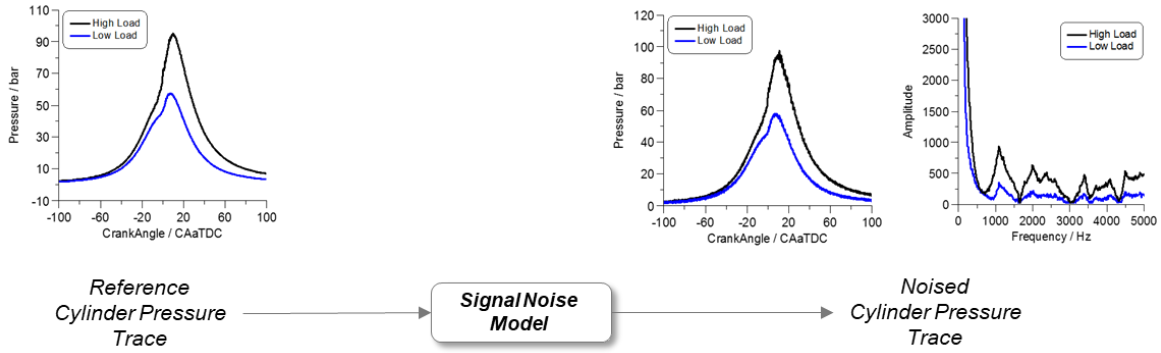

Figure 3.31: Schematic simulation of pressure signal noise for high and low load

With the new simulated pressure signal, X10 and ignition delay are calculated with the procedure described above, in order to obtain the cetane number prediction.

3.5 Summary and conclusion

Three representative fuels were tested on a 4-cylinder engine in order to analyse the combustion behaviour. From this analysis it was possible to identify the effect of fuel properties on combustion characteristics. The result obtained is the direct influence of cetane number on ignition delay and X10. However, the first parameter shows a lower sensitivity to possible disturbances that may occur in a series application. Therefore, the ignition delay has been identified as the ideal combustion characteristic for cetane number detection.

With these findings a function has been built to identify the cetane number based on the deviation of the ignition delay. In addition, based on experimental data, models of pressure sensor drift and pressure signal noise were built to verify the robustness of the function developed.

4 Function results and validation

4.1 Function

The fuel identification function can be summarised in a function activation module according to certain criteria, in the cetane number identification module, based on the ignition delay prediction sub-module. The latter, as discussed, can either be a reference value or calculated with ignition delay model. The more robust the ignition delay prediction is, the more robust the accuracy of the cetane number will be.

The function has been validated on the complete engine map for the three fuels under investigation. The 5 possible options discussed in the chapter 3.3.1 have been analyzed in order to figure out which is the most suitable method to predict the cetane number.

Option	Release Criteria	Ignition delay Reference
1.1	Engine Speed Bmep Coolant Temperature	Single value
1.2	Engine Speed Bmep Coolant Temperature	Three values
2.1	Intake pressure Intake Temperature Oxygen concentration Rail pressure Coolant temperature	Single value
2.2	Intake pressure Intake Temperature Oxygen concentration Rail pressure Coolant temperature	Three values
2.3	Intake pressure Intake Temperature Oxygen concentration Rail pressure Coolant temperature	Ignition delay Model

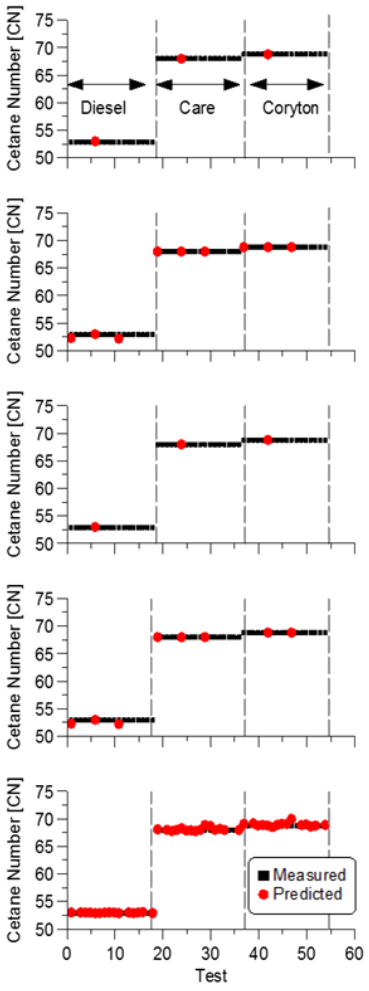

Figure 4.1: Function results for 5 release criteria

As can be seen from Figure 4.1 in the first two options, where the function is activated under specific engine operation points, the results are very accurate. In the first one the function has been

validated on the engine maps of the three fuels and we can see that the function is activated at the same operation point for the three fuels providing a correct cetane number value. In the second one the function has been activated in three different engine operation points with the same accurate result. Similarly, for options 2.1 and 2.2, the function has been validated when certain thermodynamic conditions are reached. Also in this case, an excellent accuracy of the results can be noted. In the last option the ignition delay model has been used as reference, so no constraint has been set for the release criteria of the function. It can be observed that the results obtained have a good accuracy, even if in some operational points the deviation is wide. However, if two distinct fuels are considered, the deviation does not affect the fuel identification.

The results obtained therefore have an excellent robustness in all cases. Both in the case of identification under specific engine operation points and under specific thermodynamic conditions, the function can accurately predict the cetane number and therefore the fuel. With the introduction of the ignition delay model the great advantage is to calculate the cetane number in real time. In a real case, the activation of the function under certain conditions may not occur and therefore it is not possible to identify the fuel in the engine. This makes it possible to give instantaneous information to the ECU in order to adapt the combustion strategies and have higher efficiency and lower pollutant emissions. For example, with a fuel with a high cetane number it has a shorter ignition delay, so that the ECU could change the fuel injection strategy by delaying it so that the centre of combustion is in an optimal position for maximum efficiency.

4.2 Cylinder pressure sensor drift

To determine whether the fuel identification function is robust enough against the pressure sensor drift, the latter has been simulated as described in Chapter 3.4.1.

The robustness of the function has been verified at five engine operation points for the different pressure sensor drift scenarios. For each sensor condition and each operation point, ignition delay and the new cetane number have derived with the fuel identification function. The new cetane number has been compared with the reference one as described schematically in Figure 4.2.

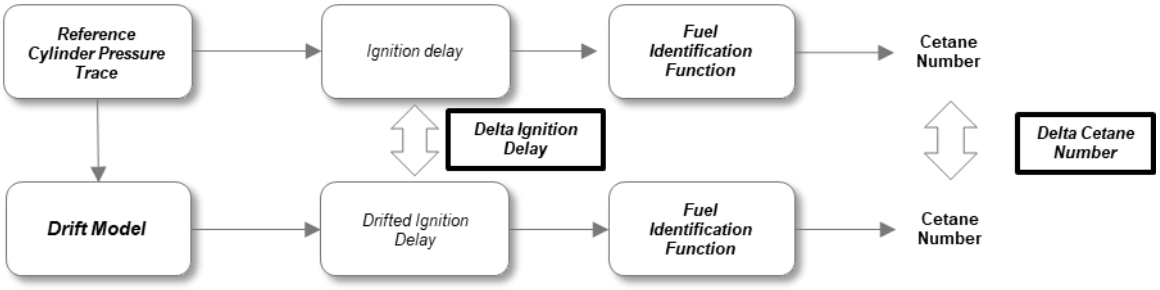

Figure 4.2: Schematic fuel identification function robustness method for cylinder pressure sensor drift

The delta of the cetane number obtained for the different drift scenarios of the pressure sensor returns the deviation that would occur in these cases and if the error is small enough to ensure fuel identification. Figure 4.3 shows the results obtained for the five engine operation points.

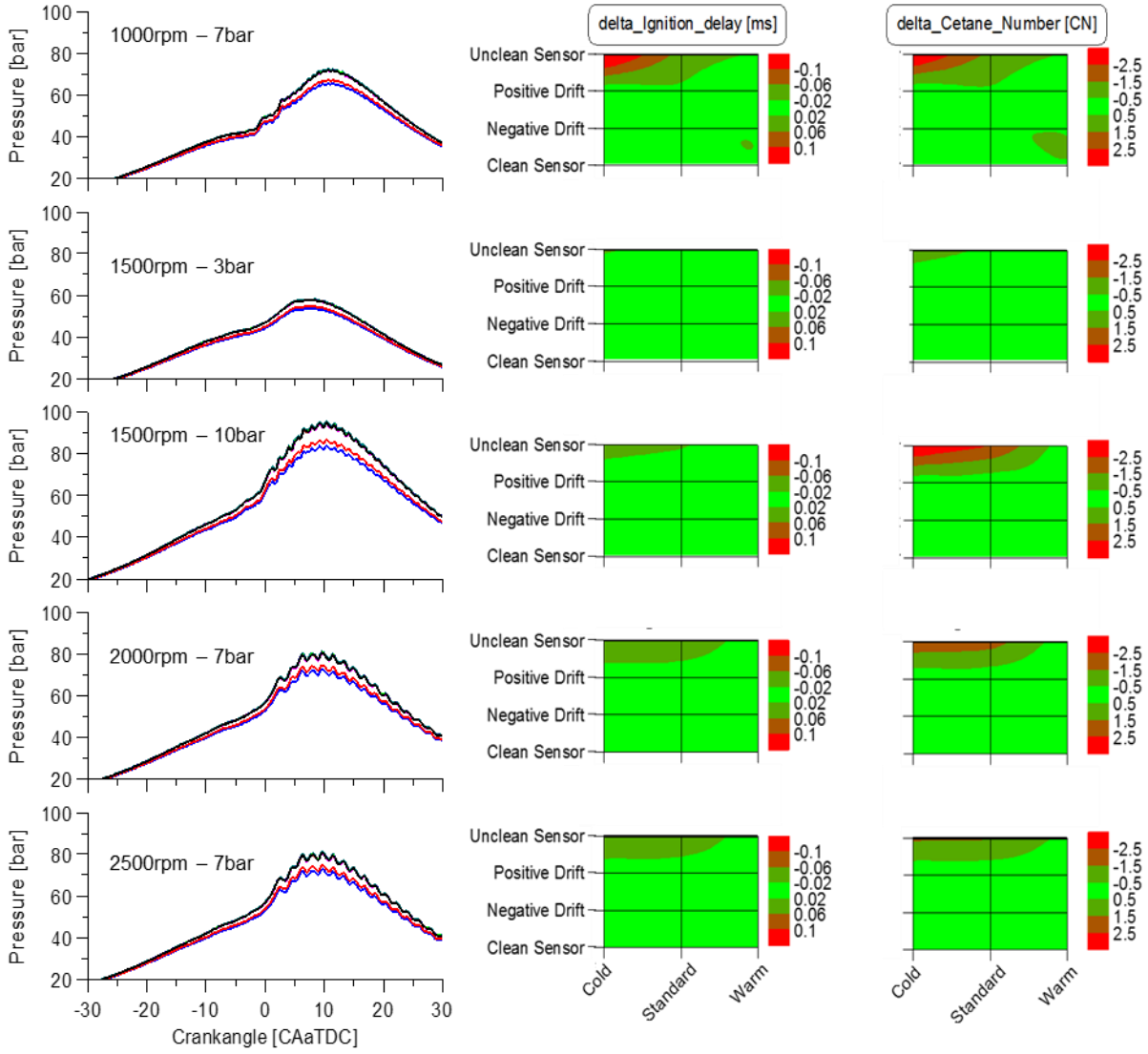

Figure 4.3: Function results with in-cylinder pressure drift

The maps show the ignition delay and cetane number deviation for the different sensor drift scenarios. The first column shows the ignition delay deviation which reaches a maximum of 0.15 ms under unclean sensor and cold condition, while under normal operating conditions the deviation is less than 0.02 ms. As a result, the cetane number deviation derived from the fuel identification function is less than 0.5 under normal operating conditions and up to 4 in the worst case of unclean sensor and cold condition. This allows to evaluate the robustness of the function in identifying the cetane number, and therefore the fuel, even with the presence of the sensor drift. In fact, considering two separate fuels, a deviation of 0.5 does not affect the detection of the cetane number.

4.3 Pressure signal noise

In addition to the pressure sensor drift, the noise signal has been simulated as described in Chapter 3.4.2. This is to further verify the robustness of the fuel identification function.

The robustness of the function has been verified in a steady state engine operation point with 100 duty cycles, since the simulation of the signal noise results in a stochastic oscillation of the ignition delay. Therefore, for each working cycle the new ignition delay and cetane number have been derived, which have been compared with the reference values, as schematically described in Figure 4.4.

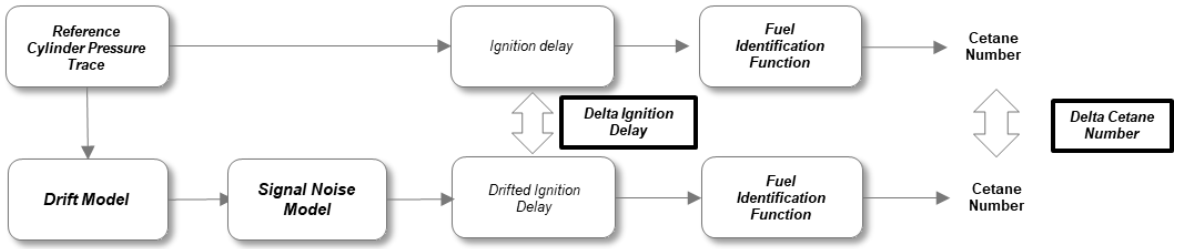

Figure 4.4: Schematic fuel identification function robustness method for pressure signal noise

The results obtained with the pressure signal noise simulation are shown in Figure 4.5. The signal noise was simulated in combination with sensor drift and in particular in thet case of unclean sensor and cold condition and in the case of clean sensor and standard condition. These two exemplary cases have been chosen to consider the worst case and the best case of sensor performance.

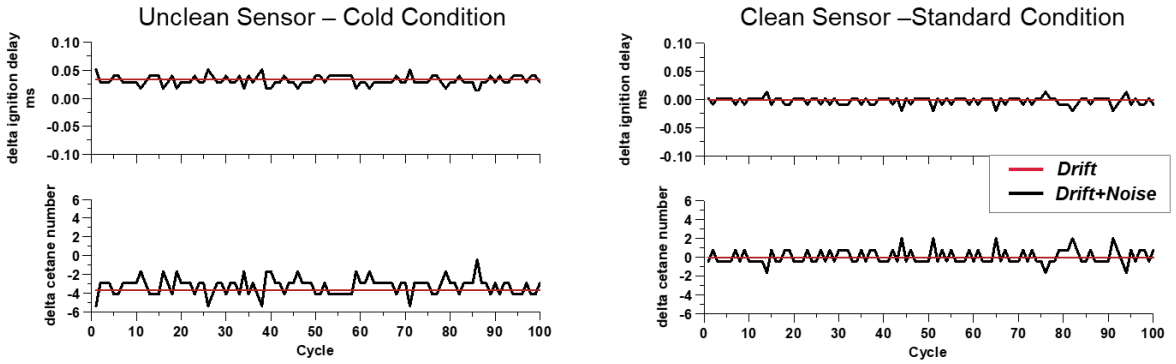

Figure 4.5: Ignition delay and cetane number deviation due to pressure signal noise (n=1500rpm bmep=10bar)

The figure shows that the presence of signal noise causes an ignition delay deviation and consequently of the calculated cetane number. This can be seen in the worst-case scenario of unclean sensor and cold condition, where ignition delay with only the presence of drift is 0.03ms while with the simultaneous presence of drift and noise it reaches 0.05ms. In the same way the cetane number has a deviation up to 5 in the presence of pressure sensor drift and signal noise.

However, under normal operating conditions, clean sensor and standard condition, the presence of signal noise causes an error in the calculation of ignition delay and cetane number, but to a smaller degree than in the worst case. In fact, the maximum ignition delay deviation reached over 100 working cycles is 0.02ms, while the maximum cetane number deviation is up to 2.

4.4 Summary and conclusion

The results obtained showed that the cetane number is identifiable by the ignition delay calculation. In fact, with the feedback of the pressure signal the combustion characteristics are calculated and through the fuel identification function developed in this work the cetane number is calculated. Moreover, the introduction of the ignition delay model has allowed a greater flexibility of the function, guaranteeing the calculation of the cetane number at any operating point. The accuracy of the function is high and ensures a calculated cetane number error of less than 2, so that it is able to identify two distinct fuels running in the engine.

The function robustness has been validated with pressure sensor drift and pressure signal noise. In fact, in series applications these disturbances may be present, so they have been simulated based on experimental data and the fuel identification function has been validated. The results of the analysis showed that the function shows good robustness in the presence of the disturbances. The presence of the pressure sensor drift alone causes the cetane number to deviate by as much as 0.5 under normal operating conditions. The simultaneous presence of pressure sensor drift and signal noise, on the other hand, leads to a cetane number deviation up to 2. This can be considered a small deviation if we consider two different fuels as those analyzed in this work. In fact Fuel 1 has a difference in cetane number of 15 compared to the reference one, so even with the presence of signal noise fuel identification function is able to identify the fuel running in the engine.

5 Outlook and future work

In current diesel engines, the cylinder pressure sensor has made it possible to analyse the combustion process. With this analysis we can derive all the combustion characteristics useful for identifying the fuel. This work has highlighted the direct influence of cetane number on ignition delay. Therefore, the fuel identification function is based on the ignition delay calculation and with appropriate calibration the cetane number can be determined. Fuel identification brings considerable advantages in terms of efficiency and pollutant emissions. The ability to identify the fuel, for multi-fuel engines, allows to adapt the combustion strategies, adopting different calibrations according to the fuel used.

The cetane number is offset by the deviation of the current ignition delay with the reference value. The current ignition delay is defined as the difference between 10 % of the burned fuel mass and the start of injection. The ignition delay reference value is obtained by means of a calculation model, which receives as input the thermodynamic properties such as temperature, pressure, oxygen concentration, to obtain the ignition delay prediction. With this method it is possible to have the flexibility of the function, which can return the cetane number value in real time, with the only constraint of steady state engine. In addition, offline validation has also demonstrated the robustness of the function in cetane number identification, ensuring a maximum cetane number deviation of 2.

However, the calculation of pressure characteristics may be affected by error. In fact, the pressure sensor from which they are calculated may suffer from disturbances such as drift or signal noise. Therefore, simulations have been carried out on these types of disturbances in order to validate the function in case of malfunction of the pressure sensor. Also in this case the function shows great robustness by returning a deviation of the cetane number up to 4, thus ensuring an effective fuel prediction in case of distinct fuels.

This work has therefore demonstrated the possibility of identifying the fuel by means of ignition delay. The results obtained show excellent robustness against pressure sensor disturbances. However, another possibility to identify the fuel is to calculate the heating value using IMEP. In fact, from previous studies, the Lower Heating Value is strongly related to the amount of fuel injected or to the BSFC. As shown in the figure, as the LHV increases, the BSFC decreases.

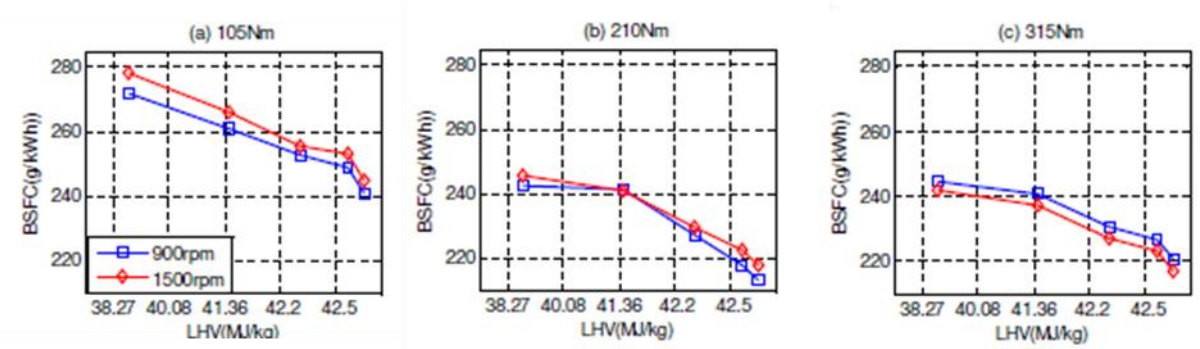

Figure 5.1: Variation of BSFC with lower heating value of biodiesel according to [43]

Moreover, the quantity of fuel is directly proportional to the IMEP value according to the formula

$$p_{IMEP} = \frac{m_f \, \eta_I \, LHV}{V}$$

Typically, the amount of fuel injected is not directly detected by a sensor, but derived from maps calibrated for engine speed and torque. Therefore, the IMEP value would be wrong according to the required torque. Its correct value can be derived from the pressure sensor and in particular from the pressure trace with the formula

$$p_{IMEP,act} = \frac{\int p \, dV}{V}$$

So, with the same concept used for ignition delay and cetane number, comparing the current IMEP value with the reference value obtained with the amount of fuel we can obtain information on LHV.

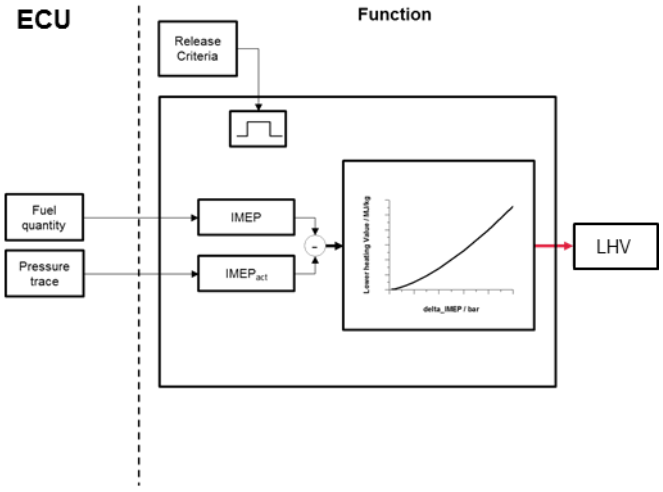

Figure 5.2: Function concept for Lower Heating Value detection

In this work it was not possible to develop this concept due to time constraints. But a detailed work on LHV could be a valid alternative to the one on cetane number. In fact, analyzing the robustness of the IMEP calculation it was very strong.

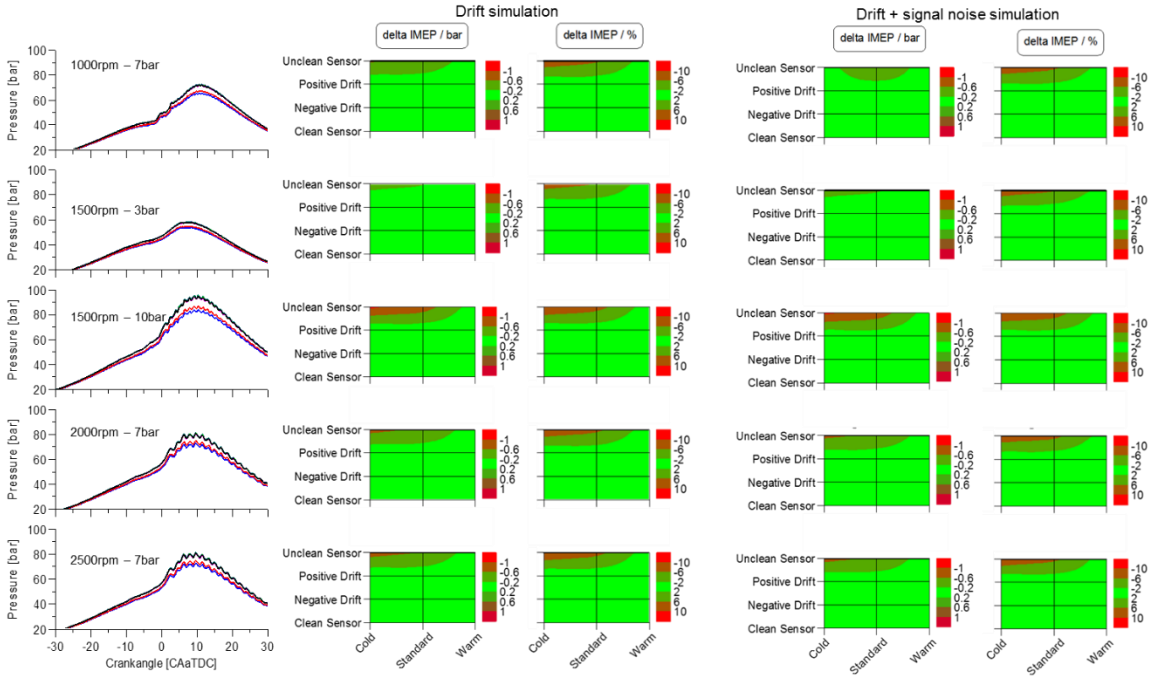

Figure 5.3: Imep deviation with pressure sensor drift and signal noise

Figure 5.3 shows how in the case of pressure sensor drift the deviation of Imep reaches 10 % in case of extreme sensor conditions in very cold temperatures, but in other cases the deviation is less than 1 %. The same applies if signal noise is added. The maximum deviation of Imep is up to 10%, but under normal operating conditions it is less than 1%.

With this it can be shown that this alternative strategy can be developed in order to identify the fuel. In fact, it can take advantage of the cylinder pressure sensor avoiding the installation of new devices or sensors.

6 References

[1] D. Hagen, «Electronic engine controls at Ford Motor Company,» SAE Technical Paper 780842, 1978.

[2] R. C. Breitzman, «Development of a Custom Microprocessor for Automotive Control,» *IEEE Control Systems Magazine,* 1985.

[3] J. H. H. a. B. H. Gerhardt, «A New Approach to Functional and Software Structure for Engine Management Systems - BOSCH ME7,» SAE Technical Paper 980801, 1998.

[4] J. a. M. K. Peyton Jones, «Automatic Calibration of 1 and 2-D Look-up Tables using Recursive Least-squares Identification Techniques,» SAE Technical Paper 2007-01-1343, 2007.

[5] Q. Weikang, «Practical solution for automotive electronic throttle control based on FPGA,» in *ICSP. 9th International Conference*, 2008.

[6] S. Pischinger, Artist, *Verbrennungskraftmaschinen I: Vorlesungsumdruck.* [Art]. RWTH Aachen, 2015.

[7] R. P., Artist, *Fundamentals of Thermodynamic for Pressure-Based Low-Temperature Premixed Diesel Combustion Control.* [Art]. University of Stuttgart, 2013.

[8] K. Siebertz, «Statistische Versuchsplanung - Design of Experiments (DoE),» 2010.

[9] J. S. C. P. S. L. M. Hinkelbein, «Control of the Diesel Combustion Process via Advanced Closed Loop Combustion Control and a Flexible Injection Rate Shaping Tool.,» SAE Int. J. Fuels Lubr., 2010.

[10] G. J. Silva, D. Aniruddha e P. B. Shankar, «PID controllers for time-delay systems.,» Springer Science & Business Media, 2007.

[11] C. Joerg, *Development of a combustion rate shaping controller for transient engine operation on a direct injection compression ignition engine.* RWTH Aachen, 2018.

[12] «Road vehicles. Calibration fluids for diesel injection equipment.». Brevetto BS ISO 4113:2010-08-31.

[13] M. Limited, Artist, *Sulphur Free Diesel BS EN 590:2013.* [Art]. 2016.

[14] Chevron, 2007. [Online]. Available: https://www.chevron.com/-/media/chevron/operations/documents/diesel-fuel-tech-review.pdf.

[15] C. Sheng e J. L. T. Azevedo, «Estimating the higher heating value of biomass fuels from basic analysis data,» in *Biomass and Bioenergy*, 2005.

[16] B. Tesfa, F. Gu, R. Mishra e A. Ball, «LHV Predication Models and LHV Effect on the Performance of CI Engine Running with Biodiesel Blends».

[17] C. Duca, «Fuel quality sensors for HD engines,» 2014.

[18] P. Heinze, «A review of analytical methods for the quantification of aromatics in diesel fuels».

[19] «ETIP Bioenergy,» [Online]. Available: http://www.etipbioenergy.eu/images/fame-fact-sheet.pdf.

[20] G. Labeckas, S. Slavinskas e A. Pauliukas, «The effect of fuel oxygen content on ignition delay and combustion of turbocharged CRDI diesel engine,» *Journal of construction and maintenance,* pp. 119-126, 2018.

[21] K. Yoshiyuki, Y. Changlin e M. Kei, «Effects of Fuel Properties on Combustion and Emission Characteristics of a Direct-Injection Diesel Engine,» 2000.

[22] E. Koehler, N. Harsha, T. Marek e T. Dean, «Impact of Fuel Properties on Light Engine Performance and Emissions,» in *Diesel Engine-Efficiency and Emissions Research (DEER)*, 2008.

[23] S. Haiwen, S. Kelly, P. Zhijun, Z. Hua e L. Nicos, «Effects of Oxygen Content of Fuels on Combustion and Emissions of Diesel Engines,» 2016.

[24] «TE Connectivity,» [Online]. Available: http://www.meas-spec.com/fluid-pro perty-sensors/fluid-property-sensors.aspx, last accessed on 2014-02-27.

[25] A. Lunati e J. Fournel, «Innovative on Board Optical Sensor Dedicated to Measure Water, Alcohols and Ethers Content in Biofuels for Flexfuel Engine Optimization,» SAE International Paper, 2008.

[26] E. Hermitte, A. Lunati e T. Delebinski, «Onboard Optimisation of Engine Emissions and Consumption According to Diesel Fuel Quality,» SAE International Paper, 2012.

[27] O. Solomon, O. A. Sunday, O. A. Kayode e O. M. Moruf, «Prediction of selected biodiesel fuel properties using artificial neural network,» 2015.

[28] E. Cheenkachorn, «Predicting Properties of Biodiesels Using Statistical Models and Artificial Neural Networks,» in *Sustainable Energy and Environment (SEE)*.

[29] W. A. Majewski, «DieselNet,» 2017. [Online]. Available: https://dieselnet.com/tech/fuel_dme.php.

[30] F. Ayala, M. Gerty e J. Heywood, «Effects of Combustion Phasing, Relative Air-fuel Ratio, Compression Ratio, and Load on SI Engine Efficiency.,» SAE Technical Paper 2006-01-0229, 2006.

[31] M. Arai, M. Shimizu e H. Hiroyasu, «Similarity between the breakup lengths of a high speed liquid jet in atmospheric and pressurized conditions.,» CLASS-91, Gaithersburg, Maryland, S. 59, 1991.

[32] W. Bergwerk, «Flow pattern in diesel nozzle spray holes.,» Proceedings of the Institution of Mechanical Engineers, 1959.

[33] J. Kim, K. Nishida e H. Hiroyasu, «Characteristics of the internal flow in a diesel injection nozzle.,» International Journal of Fluid Mechanics Research, 1997.

[34] S. Turns, An Introduction to Combustion: Concepts and Applications., Second Edition, McGraw-Hill, 2000.

[35] M. Carr, P. Caton, L. Hamilton, J. Cowart, M. Mehl e W. Pitz, «An experimental and modeling-based study into the ignition delay characteristics of diesel surrogate binary blend fuels.,» *Journal of Engineering for Gas Turbines and Power,* 2012.

[36] K. Fieweger, R. Blumenthal e G. Adomeit, «Self-ignition of SI engine model fuels: a shock tube investigation at high pressure.,» *Combustion and Flame,* 1997.

[37] K. A. Heufer e H. Olivier, «Determination of ignition delay times of different hydrocarbons in a new high pressure shock tube.,» *Shock Waves,* 2010.

[38] H. Hiroyasu e M. Arai, «Structures of fuel sprays in diesel engines.,» SAE Technical Paper, 1990.

[39] «Sensata: Data sheet - CPOS Series».

[40] M. Wlodarczyk, «High Accuracy Glow Plug-Integrated Cylinder Pressure Sensor for Closed Loop Engine Control.,» in *SAE 2006 World Congress & Exposition*, 2006.

[41] F.Payri, «New Methodology for In-cylinder Pressure Analysis in Direct Injection Diesel Engines - application to combustion noise,» Meas. Sci. Technol., 2005.

[42] J.-S. Pfluger, Artist, *Untersuchung des Optimierungspotentials der Echtzeit-Zylinderdruckauswertung durch Einsatz eines FPGA.* [Art]. RWTH.

[43] B. Tesfa, «Combustion and Performance Characteristics of CI Engine Running with Biodiesel,» Computing and Engineering, University of Huddersfield.